FAKULTA
ELEKTROTECHNICKÁ
ČVUT V PRAZE

Horn antenna enhanced by 3D printed dielectric rod

Bachelor's thesis
2022/2023

Electronics and Communications

Author:
Tyurin Roman

Supervisor
doc. Ing. Pavel Hazdra, Ph.D.
Department of Electromagnetic Field

ZADÁNÍ BAKALÁŘSKÉ PRÁCE

I. OSOBNÍ A STUDIJNÍ ÚDAJE

Příjmení: **Tyurin** Jméno: **Roman** Osobní číslo: **499295**

Fakulta/ústav: **Fakulta elektrotechnická**

Zadávající katedra/ústav: **Katedra elektromagnetického pole**

Studijní program: **Elektronika a komunikace**

II. ÚDAJE K BAKALÁŘSKÉ PRÁCI

Název bakalářské práce:

Možnosti zlepšení parametrů trychtýřové antény pomocí dielektrické tyče

Název bakalářské práce anglicky:

Horn Antenna Enhanced by 3D Printed DielectricRod

Pokyny pro vypracování:

Prostudujte možnosti vylepšení parametrů standardní trychtýřové antény dostupné na Katedře elektromagnetického pole pomocí dielektrické tyče. Zaměřte se zejména na zvýšení zisku takové antény. Vyberte vhodný dielektrický materiál, změřte jeho elektrické vlastnosti a pomocí simulátoru pole navrhněte vhodnou strukturu, která bude vytištěna na 3D tiskárně a vsazena do stávajícího trychtýře. Inovovanou anténu změřte (vyzařovací charakteristiky, zisk, přizpůsobení) a porovnejte parametry s původním trychtýřem.

Seznam doporučené literatury:

1/ LEE, Hongmin a Hyungsup LEE. A compact dielectric rod-loaded conical horn antenna for millimeter-wave apllications. In: Proceedings of 2012 5th Global Symposium on Millimeter-Waves [online]. IEEE, 2012, 2012, s. 182-185 [cit. 2022-11-30]. ISBN 978-1-4673-1305-6.
Available: doi:10.1109/GSMM.2012.6314031
2/ SATO, Keisuke, Ichiro OSHIMA a Hisamatsu NAKANO. Rod Antenna for 28-GHz Band Operation. In: 2022 IEEE-APS Topical Conference on Antennas and Propagation in Wireless Communications (APWC) [online]. IEEE, 2022, 2022-9-5, s. 012-013 [cit. 2022-11-30]. ISBN
978-1-6654-8113-7. Available: doi:10.1109/APWC49427.2022.9900007
3/ MUSTAFA, S. K. a S. YASIR. Design, development and testing of dielectric tapered rod feed for parabolic reflector antenna as an alternate to feed horns. In: Proceedings of 2013 10th International Bhurban Conference on Applied Sciences and Technology (IBCAST) [online]. IEEE, 2013, 2013, s. 369-371 [cit. 2022-11-30]. ISBN 978-1-673-4426-5. Available: doi: 10.1109/IBCAST.2013.6512181
4/ ANDO, T., ISAO OHBA, S. NUMATA, J. YAMAUCHI a H. NAKANO. Linearly and curvilinearly tapered cylindrical-dielectric-rod antennas. IEEE Transactions on Antennas and Propagation [online]. 2005, 53(9), 2827-2833 [cit.2022-11-30].ISSN 0018-926X. Available:
doi:10.1109/TAP.2005.854551
5/ SPORER, Michael, Robert WEIGEL a Alexander KOELPIN. A 24 GHz Dual Polarized and Robust Dielectric Rod Antenna. IEEE Transactions on Antennas and Propagation [online]. 2017, 65(12), 6952-6959 [cit. 2022-11-30]. ISSN 0018-926X. Available: doi:10.1109/TAP.2017.2764530

Jméno a pracoviště vedoucí(ho) bakalářské práce:

doc. Ing. Pavel Hazdra, Ph.D. FEL ČVUT v Praze, K 13117

Jméno a pracoviště druhé(ho) vedoucí(ho) nebo konzultanta(ky) bakalářské práce:

Datum zadání bakalářské práce: **08.02.2023** Termín odevzdání bakalářské práce: **26.05.2023**

Platnost zadání bakalářské práce: **22.09.2024**

doc. Ing. Pavel Hazdra, Ph.D. podpis vedoucí(ho) práce	podpis vedoucí(ho) ústavu/katedry	prof. Mgr. Petr Páta, Ph.D. podpis děkana(ky)

III. PŘEVZETÍ ZADÁNÍ

Student bere na vědomí, že je povinen vypracovat bakalářskou práci samostatně, bez cizí pomoci, s výjimkou poskytnutých konzultací. Seznam použité literatury, jiných pramenů a jmen konzultantů je třeba uvést v bakalářské práci.

.	
Datum převzetí zadání	Podpis studenta

Author statement for undergraduate thesis

I declare that the presented work was developed independently and that I have listed all sources of information used within it in accordance with the methodical instructions for observing the ethical principles in the preparation of university theses.

Prague, date ....

Signature

Acknowledgements

I would like to express my sincere gratitude to my thesis supervisor, doc. Ing. Pavel Hazdra, Ph.D., for his invaluable guidance, patience, and support throughout the entire research process. His vast knowledge and expertise in the field of antenna design have been instrumental in the completion of this work.

I am also grateful to Ing. Tomáš Kořínek, Ph.D., who provided me with technical assistance and expertise in manufacturing the dielectric rod for my experiments.

I would like to extend my appreciation to my colleague, Ing. Vratislav Sokol, Ph.D., for his insightful discussions and valuable suggestions that have helped me to broaden my understanding of the subject.

Finally, I would like to thank my family for their unwavering support and encouragement throughout my academic journey. Their love and encouragement have been a constant source of motivation and inspiration for me.

Abstract

Dielectric rod that enhances parameters of a horn antenna is presented in this thesis. The rod was design for a WR187 horn operating in the frequency range of 3.95 to 5.85 GHz. To achieve more precise results while simulating the rod, the material of the rod was extracted using waveguide measurements. The final model of the rod was printed, and both the horn and the horn with the dielectric rod were measured. After analyzing the measured data, it was found that the rod increased the antenna gain by an average of 5 dB. Reflection coefficient of enhanced antenna has also been improved and is below -17 dB across its entire frequency range. Radiation pattern indicates that antenna is more directional than before.

Index terms—Antenna, waveguide, horn antenna, dielectric loading, dielectric rod, tapered rod

Abstrakt

V této práci je prezentována dielektrická tyč, která vylepšuje parametry trychtýřové antény. Tyč byla navržena pro trychtýř standardu WR187, jehož provozní pásmo je 3,95 až 5,85 GHz. Aby se dosáhlo přesnějších výsledků simulace, materiál, ze kterého se tyč vyrobila, byl extrahován měřením na vlnovodu. Finální model tyče byl vytištěn a proběhlo měření jak trychtýře samotného tak i se vsunutou dielektrickou tyčí. Po analýze měření se ukázalo, že tyč způsobila navýšení zisku průměrně o 5 dB. Činitel odrazu upravené antény se také vylepšil a je v celém jejím frekvenčním pásmu pod -17 dB. Anténa je směrovější než předtím, na což poukazují změřené vyzařovací diagramy.

Klíčová slova— Anténa, vlnovod, trychtýřová anténa, dielektrická tyč, zúžená tyč.

Contents

List of Figures

List of Tables

List of Abbreviations and symbols

Abbreviation/Symbol	**Definition**
UHF	Ultra High Frequencies
CST	3D EM analysis software package
SWR	Standing wave ratio
Γ	Reflection coefficient
Z_{a}	Impedance of antenna
λ	Wavelength
G	Gain
PTFE	Polytetrafluorethylen
η	Impedance of a space
e	Aperture efficiency
FSL	Free Space Loss
f	Frequency
P	Power
α	Attenuation rate
TRL	True Reflect Line
VNA	Vector network analyzer
PEC	Perfect electric conductor
WR187	Rectangular waveguide standard (1.872 inches x 0.872 inches)

Introduction

An antenna is a device used to transmit or receive electromagnetic waves. It converts current energy to electromagnetic waves energy and vice versa. Today, there are many different types of antennas that are divided based on construction parameters, fields of application, and operating frequency range, among other factors.

To characterize an antenna, certain parameters must be known, which will be presented in the upcoming chapters. These parameters can be determined in two ways: through simulation using software such as CST or through measurement using two antennas: a transmitting antenna and a receiving antenna. The transmitting antenna's parameters are the ones we want to determine, while the **Horn antenna** is typically used as the receiving antenna.

A Horn antenna is widely used at UHF[1] and microwave frequencies. Usually, this type of antenna is used in gun radars, automatic door openers etc. As it was mentioned earlier it can be also used for measurement.

Main advantages of horn antenna are:

- Directivity,
- Simple to construct,
- High gain,
- Good impedance matching.

Although it has good directivity and high gain, in some cases there are requirements for higher gain or narrow beam-width. For instance to use in medicine as it was mentioned in [1] or point-to-point communication and satellite communication mentioned in [2]. In both articles dielectric rod was inserted to achieve increase in gain of antenna or modify its radiation pattern, makes it narrow, suppress cross-polarization and etc.

For these purposes we will attempt to design dielectric rod for WR187 antenna that has operating frequency range between 3.95 GHz and 5.85 GHz. However it will be necessary to understand the fundamentals of electromagnetic wave propagation, which will be shown in the next section. Then we are going to speak about construction of the rod and some tapered parts of the rod, which were mentioned in [3] and [5]. Once the rod is designed and simulated, it will be manufactured and measured. Finally, the antenna with the rod and without it will be compared to determine the effectiveness of the modifications.

[1] Ultra High Frequencies (UHF) is a range of frequencies between 300 MHz and 3 GHz

Chapter 1

Antennas characterization

1.1 Parameters

In this section, some antenna parameters that can be used to characterize any antenna and its pattern of electromagnetic field are presented.

- The range of frequencies on which antenna can radiate efficiently is called **Bandwidth**.
- The **efficiency** of antenna, which is defined as the ratio of the radiated power to total power input to the antenna, is affected by power losses. These losses can be due to heating effects, as well as reflected power.
- Power reflection is a common phenomenon on microwave frequencies and is usually expressed by the so-called **reflection coefficient** or by the parameter called **standing wave ratio (SWR)**. Both parameters describe the same thing and are related by the following formula:

$$\mathrm{SWR} = \frac{1 + |\mathbf{\Gamma}|}{1 - |\mathbf{\Gamma}|}, \tag{1.1}$$

  where $|\mathbf{\Gamma}|$ the magnitude of the reflection coefficient, which is defined as the absolute value of the ratio of the reflected wave amplitude to the incident wave amplitude.
- **Gain** or **power gain** is the ratio of radiation intensity in a given direction to the radiation intensity that would be produced by an isotropic antenna [1]. **Directivity** is the ratio of the radiation intensity in a given direction to the radiation intensity averaged over all directions. Both parameters are expressed in dB and describe the radiation pattern of the antenna.
- **Impedance** of antenna, $\boldsymbol{Z_a}$, is also an important parameter, especially for calculating radiated power and for achieving impedance matching.

More detailed information about antennas parameters can be found [8].

[1] Isotropic antenna radiate the same power density in all directions.

1.2 Approximate equations

In this section approximate equations for a pyramidal horn antenna will be presented. Also gain of the used horn will be calculated. In figure 1.1 the dimensions of the used pyramidal horn are presented.

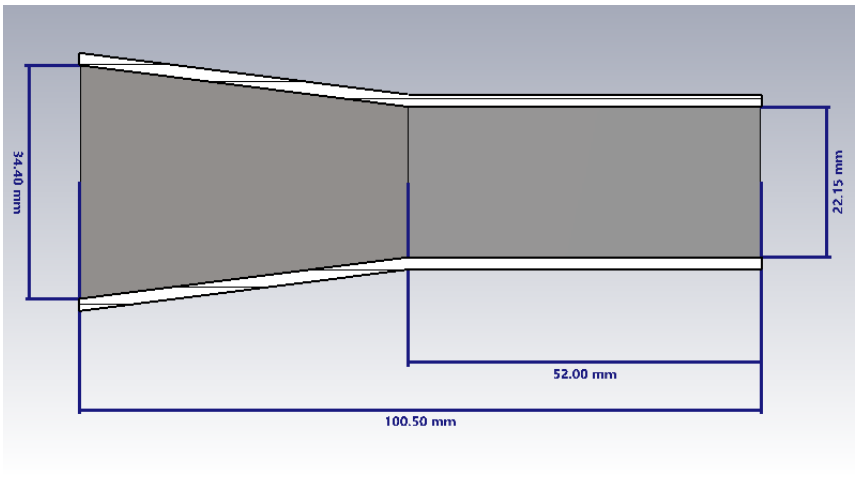

(a)

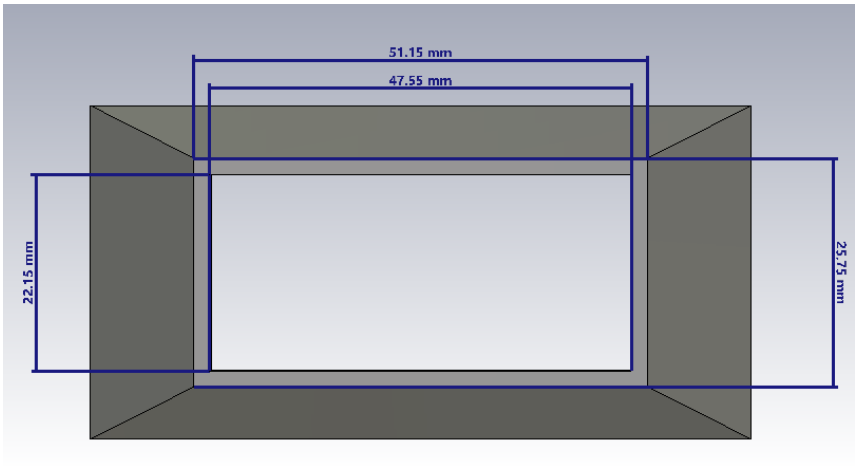

(b)

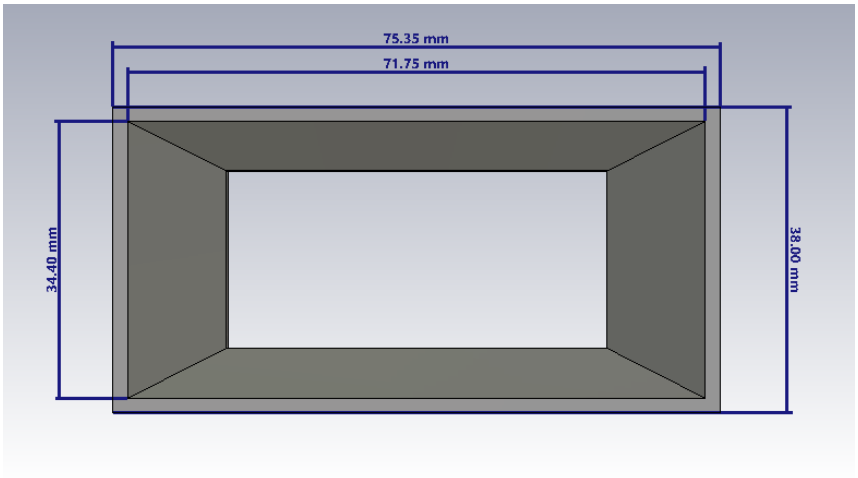

(c)

Figure 1.1: Dimensions of used horn.

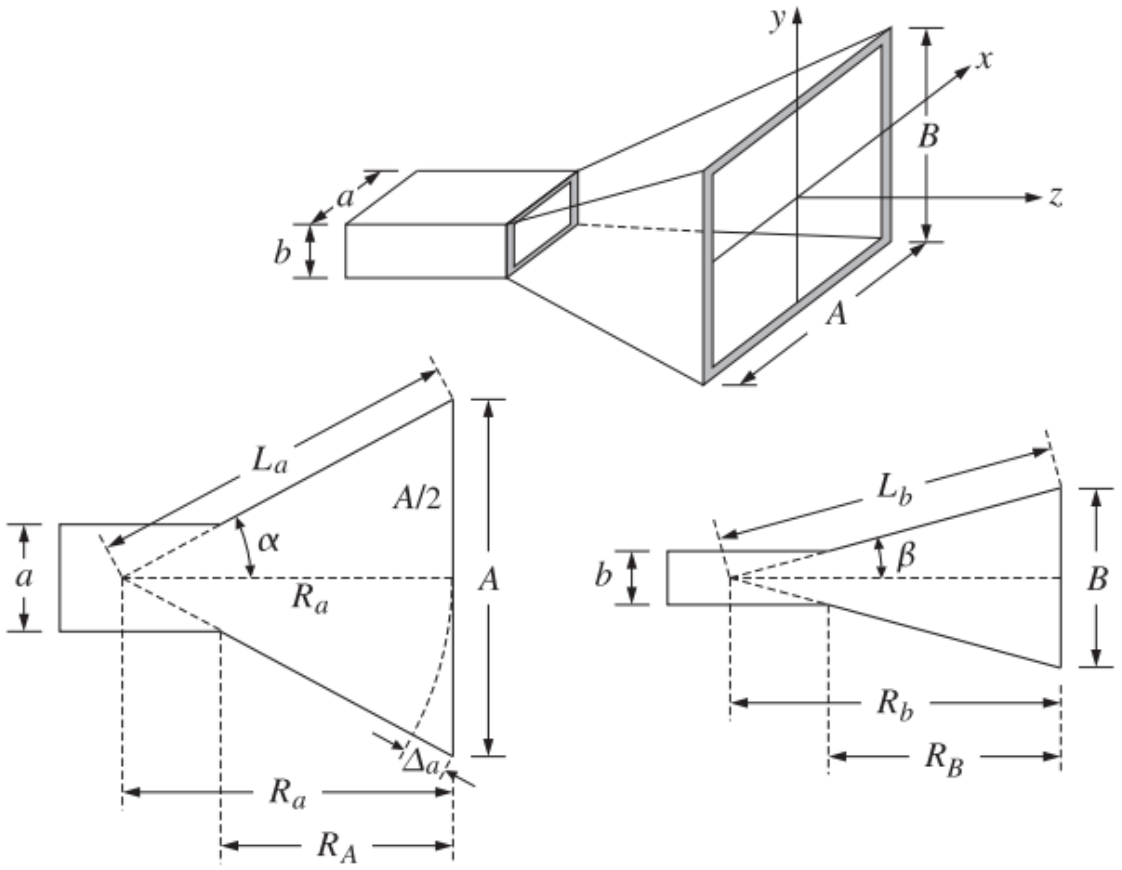

Figure 1.2: The geometry of the pyramidal horn from [8].

Parameters on the figure 1.2 will be used to calculate gain of used horn. Therefore, $A = 71.75$ mm, $B = 34.4$ mm, $a = 47.55$ mm and $b = 22.15$ mm. For pyramidal horn parameters R_A and R_B should be equal, they represent perpendicular distances from the plane of the waveguide opening to the plane of the horn. For used horn $R_A = R_B = 48.5$ mm. Knowing these parameters makes possible to calculate R_a and R_b using next formula:

$$R_a = \frac{A}{A-a} R_A = 143.8 \text{ mm}, \tag{1.2}$$

$$R_b = \frac{B}{B-b} R_B = 136.2 \text{ mm}. \tag{1.3}$$

At the next step σ_a and σ_b should be calculated:

$$\sigma_a^2 = \frac{A^2}{2\lambda R_a}, \tag{1.4}$$

$$\sigma_b^2 = \frac{B^2}{2\lambda R_b}, \tag{1.5}$$

where λ is wavelength. Then, aperture electric (1.6) and magnetic field (1.7) can be

calculated using next formula:

$$E_y(x,y) = E_0 \cdot \cos\left(\frac{\pi x}{A}\right) \cdot \mathrm{e}^{-\mathrm{j}(\pi/2)\sigma_a^2(2x/A)^2} \cdot \mathrm{e}^{-\mathrm{j}(\pi/2)\sigma_b^2(2y/B)^2}, \tag{1.6}$$

$$H_x(x,y) = -\frac{E_y(x,y)}{\eta}, \tag{1.7}$$

where η is impedance of a space.

Now, it is possible to compute gain of antenna. Frequency range for the horn is 3.95 to 5.85 GHz. Formula for calculating maximum gain is:

$$G = e \cdot \frac{4\pi}{\lambda^2} \cdot A \cdot B, \tag{1.8}$$

where e is aperture efficiency and can be calculated using σ_a^2, σ_b^2 and Fresnel function. Detailed detachment of all formulas and MATLAB script for calculation of gain and directivity can be found in [8].

Graph of gain over frequencies from eq. (1.8) is shown below:

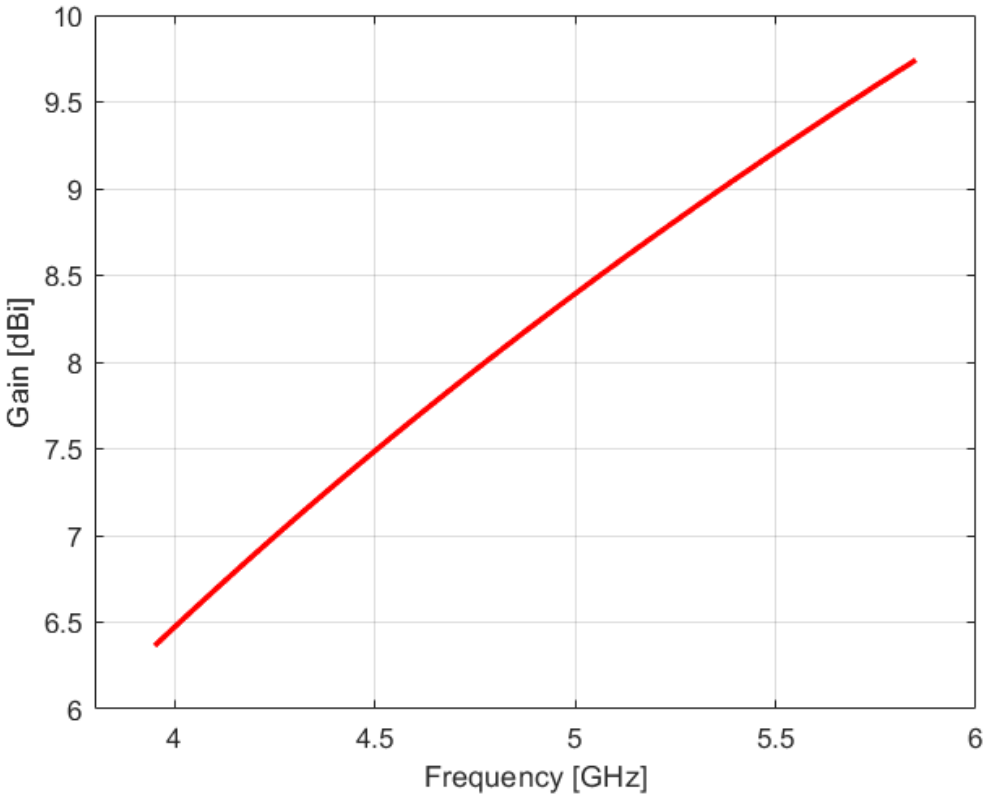

Figure 1.3: Calculated maximum gain of used horn.

1.3 Characterization of radiation pattern

One of an antenna's most crucial qualities is its radiation pattern, which shows how much energy is radiated in various directions. The analysis of how the radiation pattern changes following the insertion of a dielectric rod is essential to this thesis. It is crucial to comprehend some of the factors that make it easier to compare radiation patterns. We can identify any potential nulls or lobes in the radiation pattern, as well as the directionality and effectiveness of an antenna, by examining the radiation pattern. This knowledge is crucial for antenna design and optimization in a variety of applications, including satellite systems, radar systems, and communication systems. In general, radiation pattern measurements are essential for comprehending an antenna's performance and possibilities.

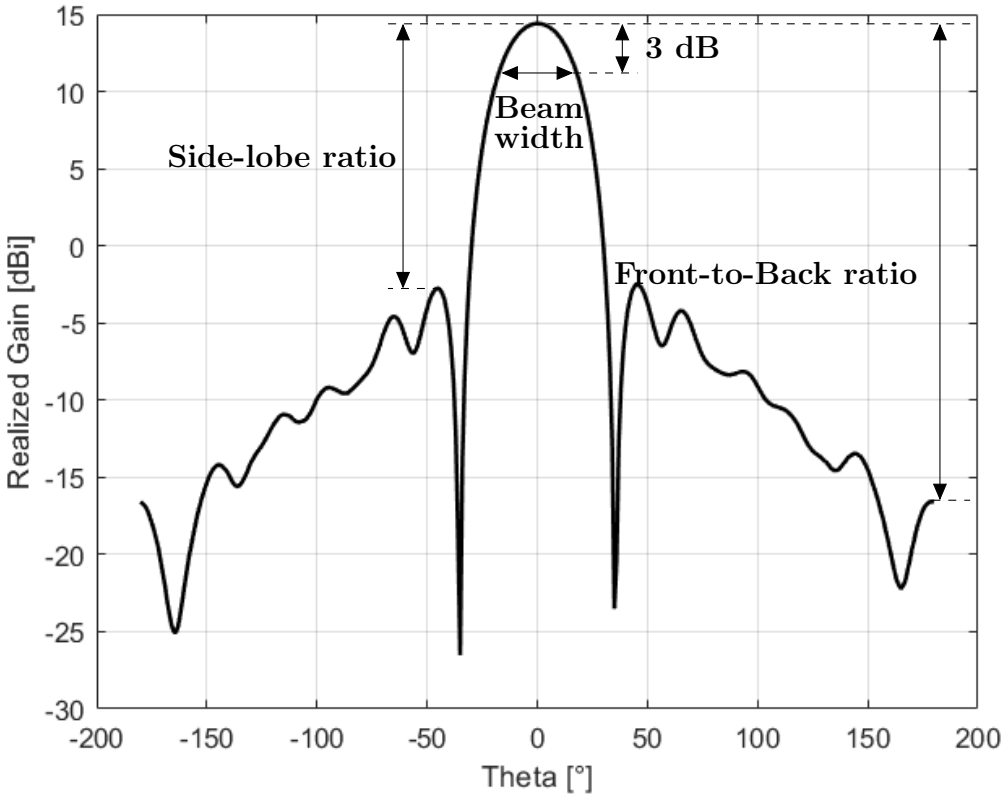

Figure 1.4: Radiation pattern.

Fig. 1.4 shows the radiation pattern of an antenna. Several parameters are needed to fully characterize it. The horizontal axis represents the angle, and the vertical axis represents the realized gain. The first important parameter is beam width, which is the angle range where the most power is radiated. Typically, it is measured for a 3 dB decrease from the peak of the main beam[2]. The second parameter is side-lobe ratio, which is defined as the ratio of the highest side-lobe power to the peak power of the main lobe. The last parameter is front-to-back ratio, which indicates how much energy is radiated backwards and is defined as the ratio of peak power radiated upwards to power radiated backwards.

[2]In this thesis, we will measure the beamwidth for a 3 dB decrease, but it can also be measured for a 6 dB and 10 dB decrease

Chapter 2

Dielectric rod design

2.1 Rod design

In this section, we will discuss the principle of designing a rod for an antenna. Inserting a dielectric material inside the antenna creates a discontinuity because an electromagnetic wave is initially excited in air and then propagates inside the waveguide until it encounters the dielectric material. The transition from air to dielectric material causes reflection, leading to aggravated radiation. To solve this problem, we must ensure a smooth transition between the two materials. This problem is discussed in articles [3], [5], and [6], and different types of tapering are used, such as linear and curvilinear. Both types can ensure good impedance matching. However, in this thesis, we decided to use exponential tapering, as presented in [6].

On the upcoming picture 2.1, an exponentially tapered part is presented. Its shape can be adjusted by two parameters: the "steepness" and the "start" of the tapered part. These two parameters will be needed for the optimization process.

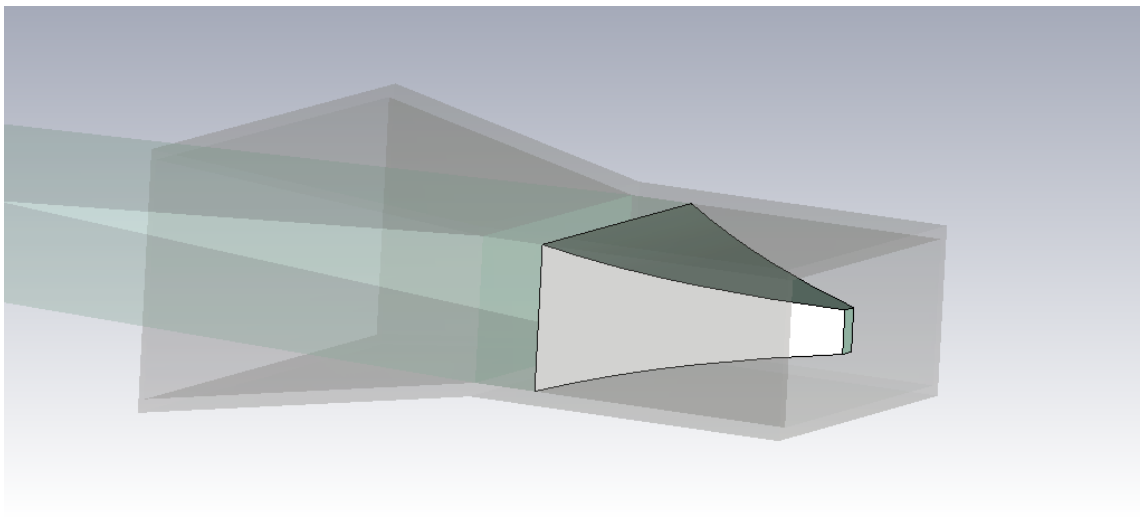

Figure 2.1: Exponential tapering.

The second part of the rod (Fig. 2.2) is designed as a dielectric brick without any tapering. The main purpose of this part is to hold the rod inside the horn of the antenna, providing mechanical support and stability. It was assumed that the length of this brick should be at least 10 mm to meet these mechanical requirements.

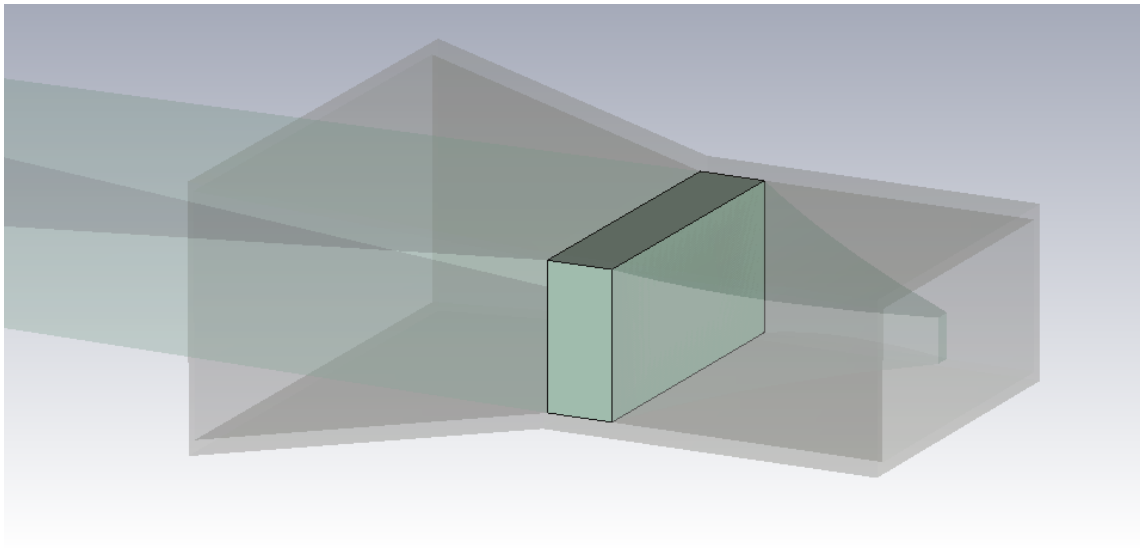

Figure 2.2: Transition part.

The third part (Fig. 2.3) consists of a transition between the dielectric material and air and is designed with linear tapering. Initially, an attempt was made to apply the same exponential tapering, but it resulted in a negative effect on the standing wave ratio (SWR) and radiated power. Therefore, through experimentation, it was discovered that this part should be tapered linearly.

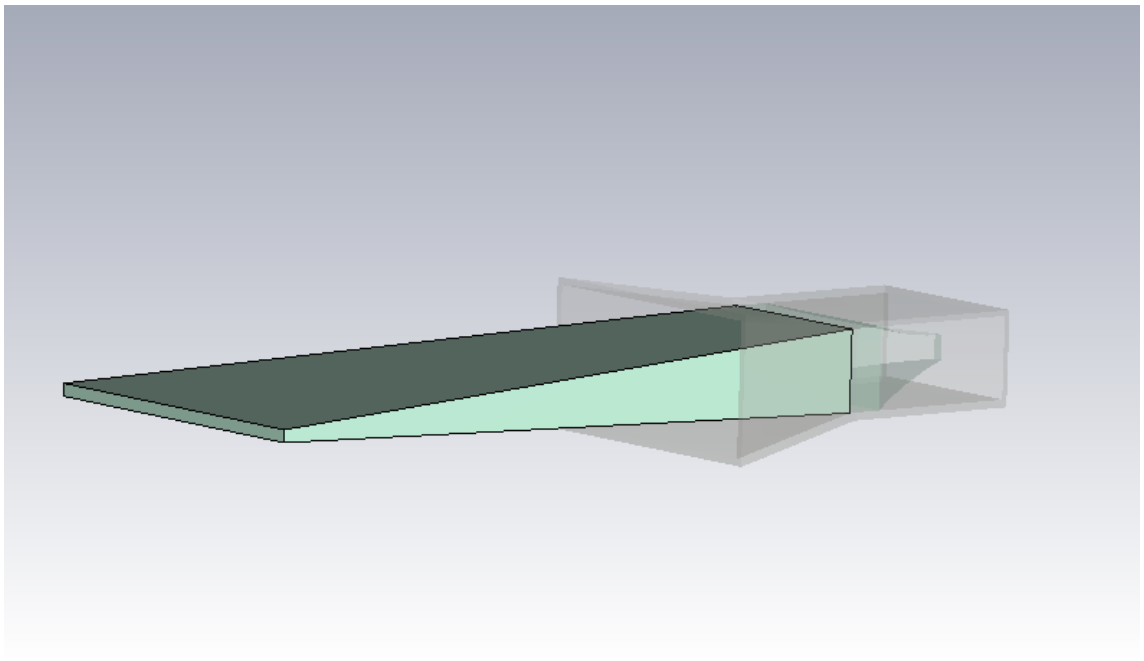

Figure 2.3: Linear tapering.

On the picture 2.4 the final rods shape is presented.

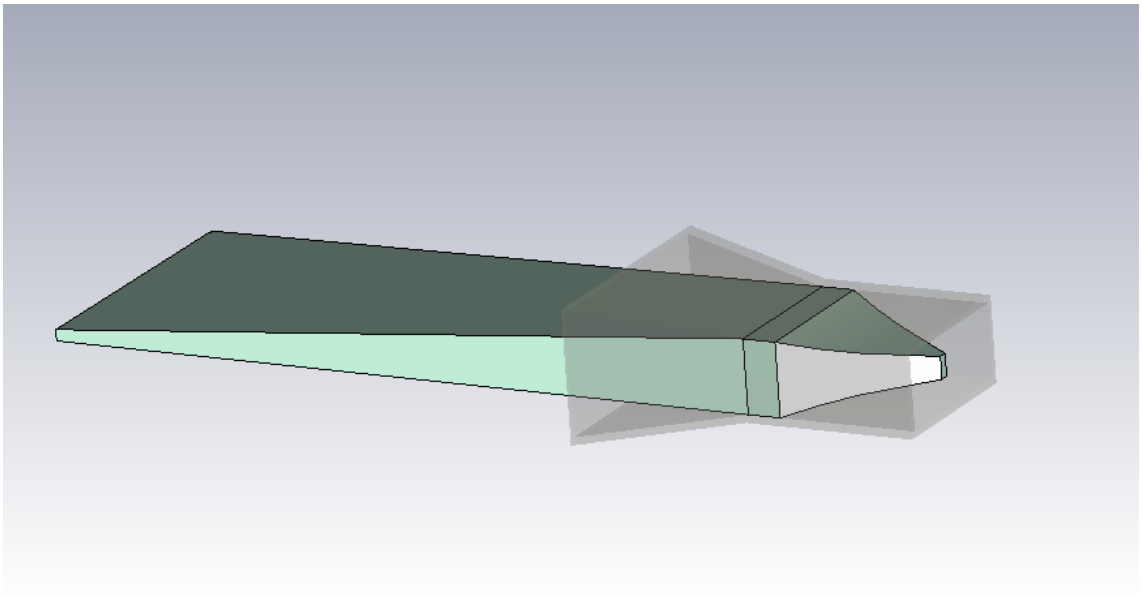

Figure 2.4: The dielectric rod prototype.

2.2 Optimization of rod parameters

The theoretical part presents several equations that can be used to calculate the electric and magnetic fields and the gain of a horn antenna. However, these equations are based on certain approximations and do not take into account the impact of the dielectric rod. Therefore, simulation software such as CST[1] is typically used for these purposes.

The designed rod also needs optimization, and the *Trust regions* algorithm was used for this purpose. For problems such as the design of a dielectric rod, it is better to perform the optimization process in two steps. In the first step, the reflection coefficient was optimized. Then, the gain of the antenna was added to the optimization, and both parameters were optimized simultaneously. The results are shown in the upcoming pictures 2.5.

[1]CST is software developed by Simulia and used for designing, analyzing and optimizing electromagnetic components and systems

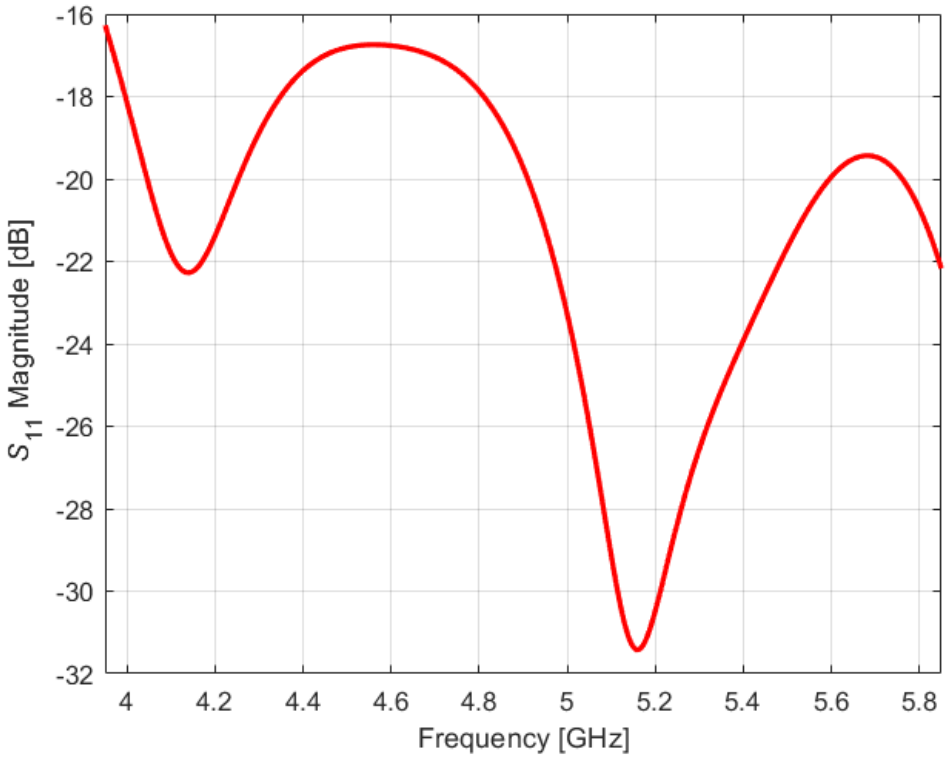

(a) S_{11} of optimized rod.

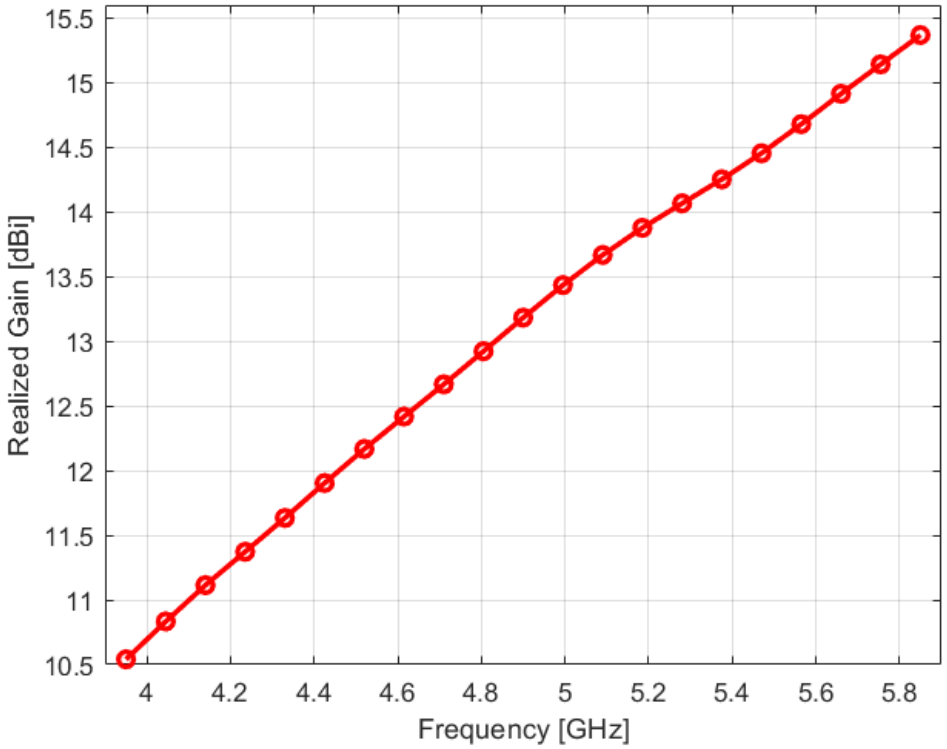

(b) Realized gain.

Figure 2.5: Results after optimization.

2.3 Material extraction

In the previous section, we presented the design of the rod, which was optimized and simulated using CST software. Now, it is necessary to manufacture the rod using realistic materials. To apply the properties of the realistic material to the antenna model, a *material extraction* process is required. In this section, we provide a brief description of the extraction method. A more detailed process with formulas can be found in [7]. The used material is called Polyamide PA12. The material extraction was performed using a vector network analyzer and waveguides with lengths of 10 mm, 20 mm, 50 mm, 100 mm, and a "Reflect" standard.

Figure 2.6: Standards 10 mm, 20 mm, 50 mm, 100 mm and "Reflect".

At the beginning of the measurement, the vector analyzer must be calibrated using the 10 mm and 20 mm waveguides as well as the "Reflect" standard. Then, the 50 mm and 100 mm waveguides were measured without the dielectric material, and in the next step, the measurement with the loaded dielectric was performed. The S-parameters of the waveguide with the dielectric are shown in the picture below (Fig. 2.7).

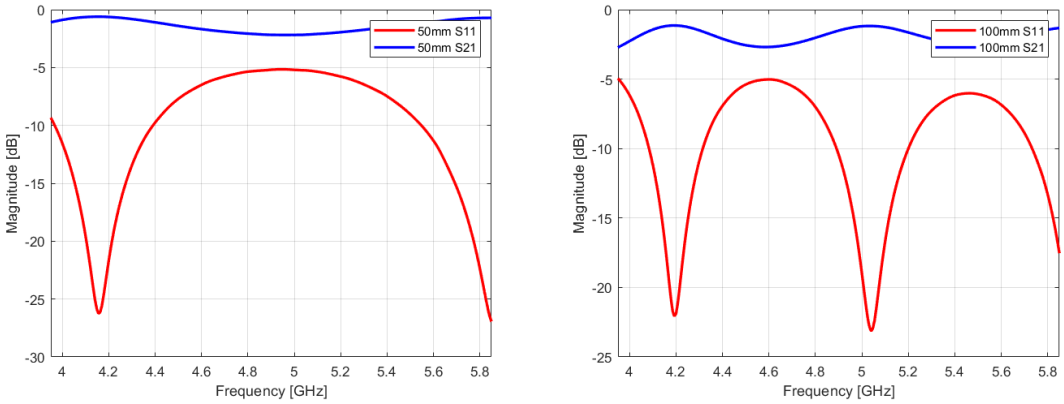

(a) (b)

Figure 2.7: S-parameters of (a) 50 mm and (b) 100 mm waveguides loaded with dielectric sample.

Finally, the complex permittivity was extracted using the implemented function in CST, as shown in Fig. 2.8.

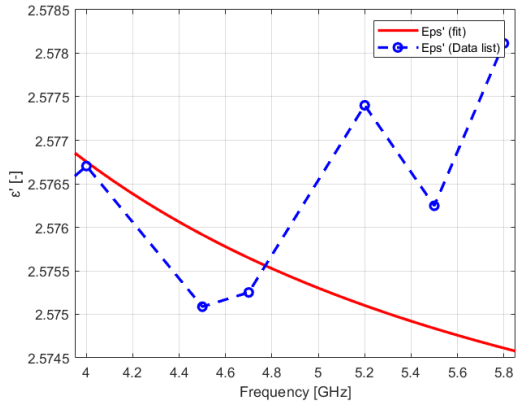

(a)

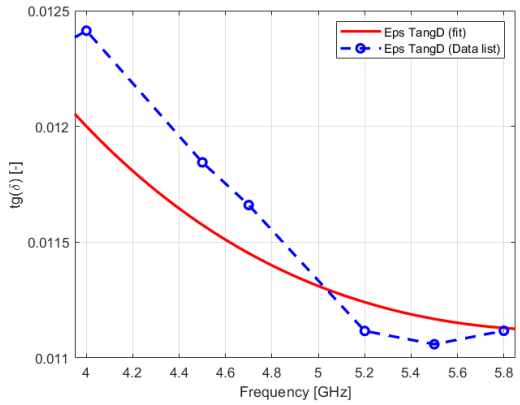

(b)

Figure 2.8: Extracted complex permittivity.

Chapter 3

Realistic antenna design

3.1 Effect of lossy material

After examining the graphs of the extracted complex permittivity, it became apparent that the material is lossy and will have a significant impact on the antenna's parameters. Therefore, once the material properties were included in the simulation, another optimization was necessary. The upcoming pictures show the reflection coefficient (Fig. 3.1), gain over frequencies (Fig. 3.2), and the final shape of the rod (Fig. 3.3) after the optimization process.

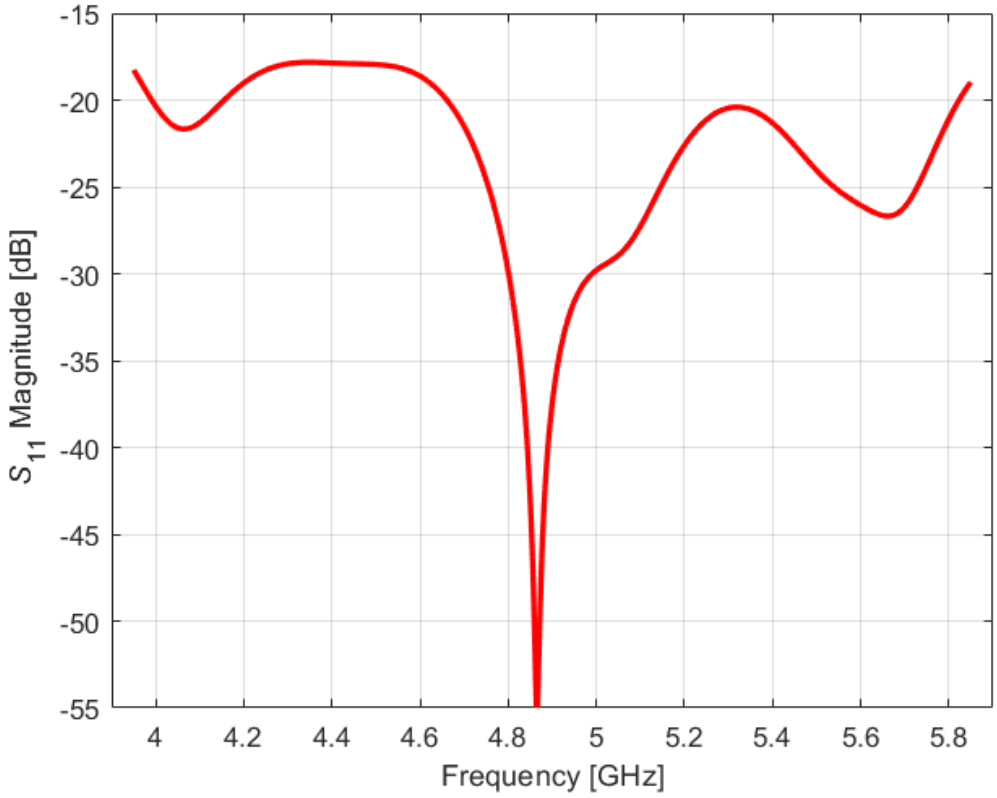

Figure 3.1: Reflection coefficient (S_{11}).

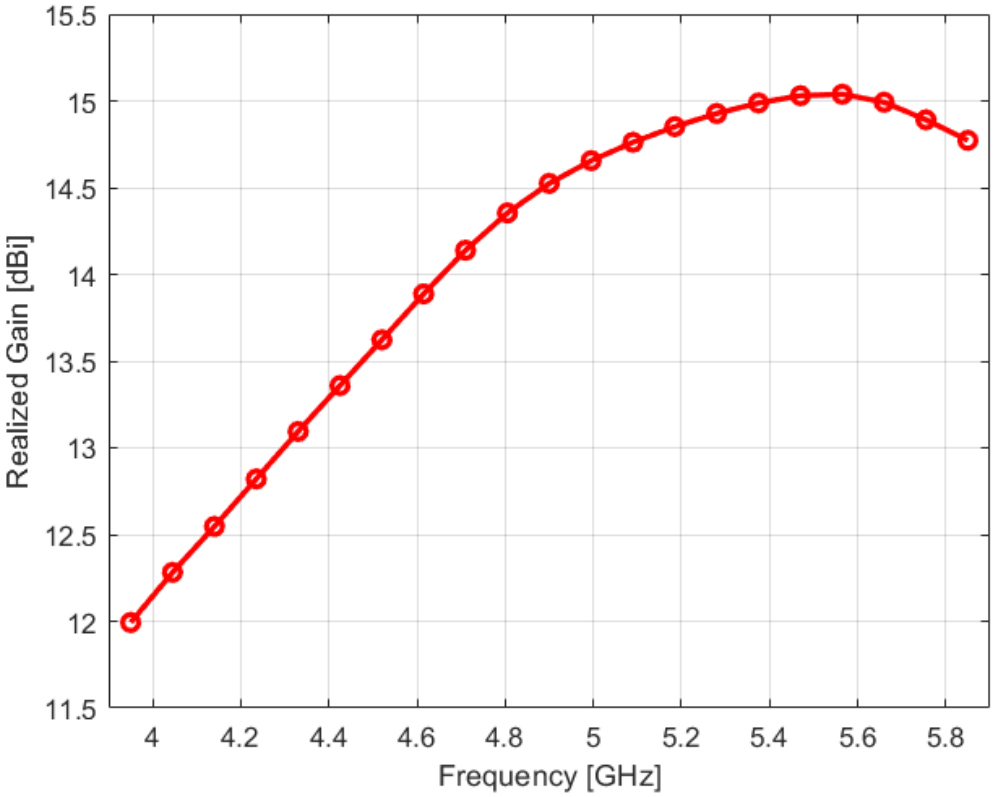

Figure 3.2: Gain over frequencies.

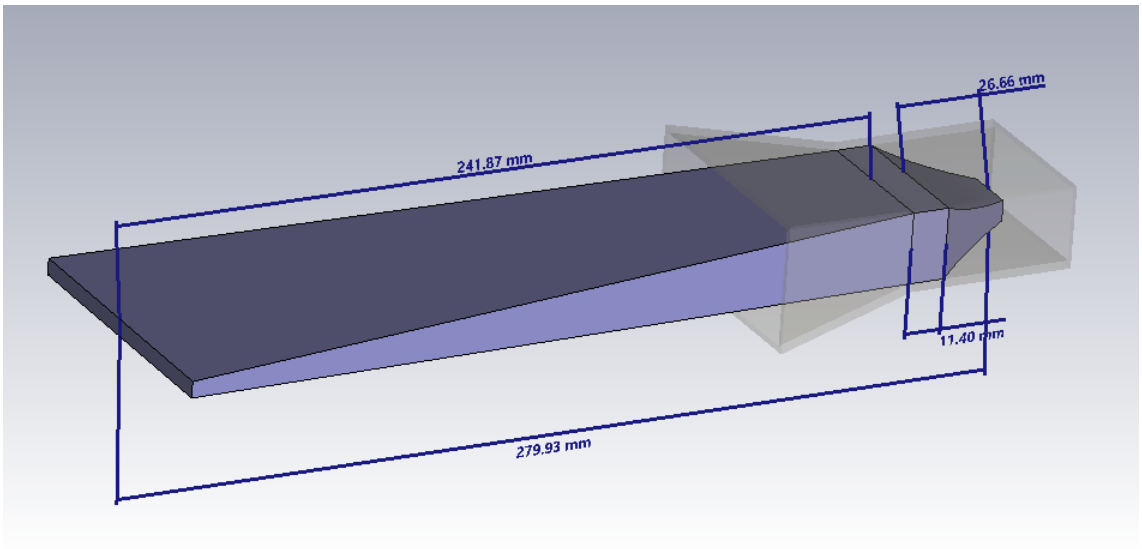

Figure 3.3: Shape of the rod.

3.2 Simulation results analysis

After completing all measurements and simulations we can compare results. In this section three models are being compared: horn antenna without rod, with rod made of PTFE (Teflon) and rod made of real "lossy material" (Polyamide PA12). First graph shows reflection coefficient of 3 models (Fig. 3.4).

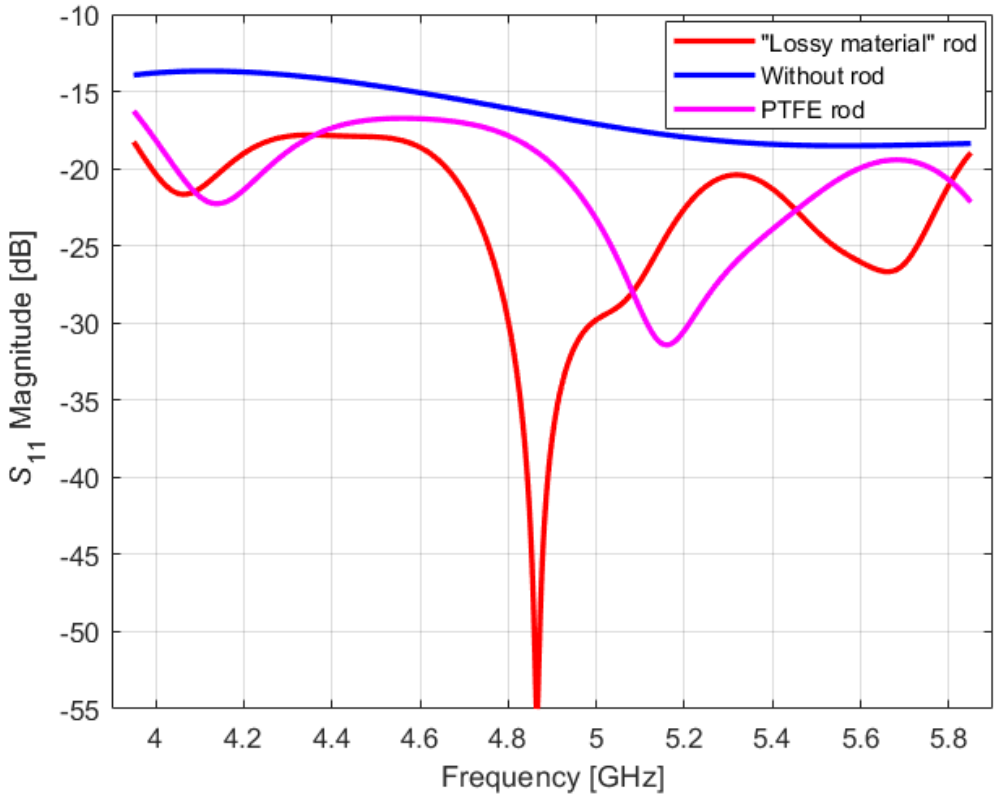

Figure 3.4: Reflection coefficient comparison.

Models that were enhanced by the dielectric rod have better impedance matching, which means less power is reflected by the structure. To achieve the highest gain, it was necessary to ensure that the reflection coefficient was as low as possible. For the "lossy material," this requirement was stricter due to losses in the material. During the optimization process, we aimed to achieve $|S11|_{\mathrm{dB}} < -20$ dB.

In the next table (Table 3.1), the maximum realized gain is shown at the start and end frequencies of the range and also the center frequency. A graph comparing all three cases (without rod, PTFE rod, and "lossy material" rod) is shown in Fig. 3.5.

Table 3.1: Maximum of realized gain on different frequencies.

Frequency [GHz]	3.95	4.90	5.85
Gain of antenna with "Lossy material" rod [dBi]	12.11	14.52	14.77
Gain of antenna without rod [dBi]	7.30	8.84	10.10
Gain of antenna with PTFE rod [dBi]	10.54	13.18	15.37

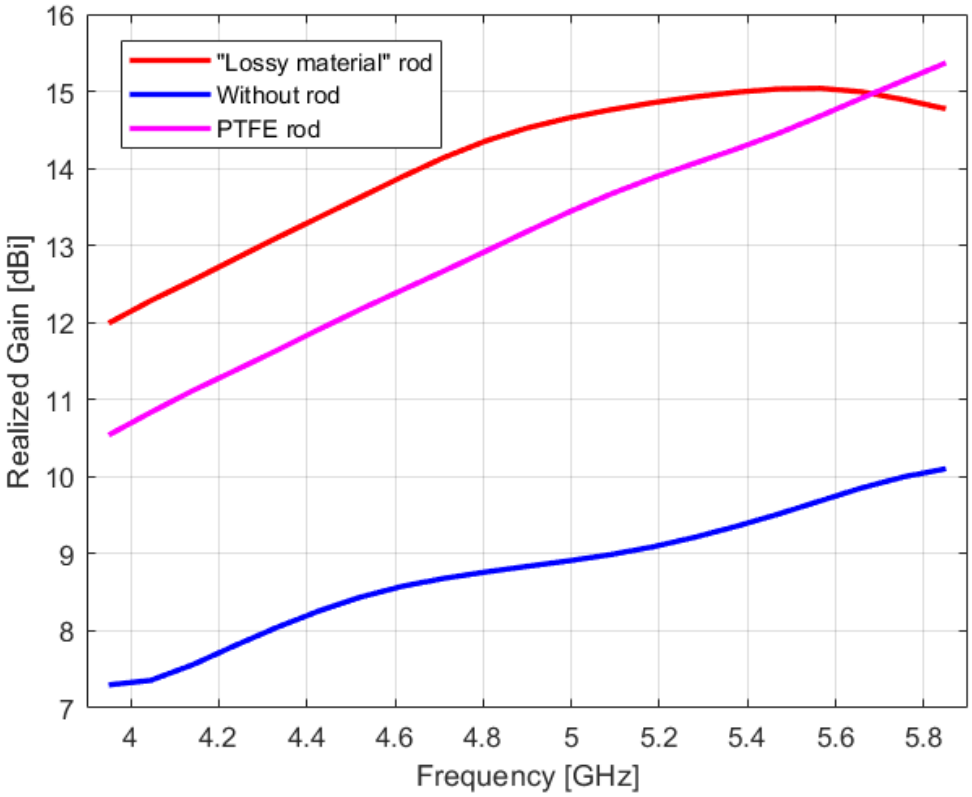

Figure 3.5: Maximum of realized gain on different frequency.

As predicted in the previous chapter, the lossy material has a significant impact on the antenna's gain. Although this impact is mainly observed in frequencies above 5.5 GHz, the "Lossy material" rod still provides a better gain compared to the PTFE rod. The PTFE rod approximately increases the gain by 4 dB compared to the antenna without a rod, while the "lossy material" rod provides an increase of approximately 5 dB in gain.

Chapter 4

Rod realization and measurements

4.1 Measuring system

After the dielectric rod was manufactured (see Fig. 4.9) using a 3D printer, it is necessary to verify if the parameters of the antenna will be improved as designed. For this purpose, the upcoming measuring system will be used:

Figure 4.1: Measuring system: block scheme.

where $\alpha \cdot l_1$ and $\alpha \cdot l_2$ are cable attenuation, G_x is gain of transceiver antenna and G_r is gain of receiving antenna. Also there is a parameter **Free Space Loss (FSL)** that was not mentioned earlier. This parameter quantifies the amount of power that is attenuated between two antennas due to the spreading of the electromagnetic wave in free space. The FSL can be calculated based on the wavelength λ and the distance d between the two antennas:

$$\mathrm{FSL} = \left(\frac{4\pi d}{\lambda}\right)^2. \tag{4.1}$$

An important condition for the formula above (4.1) to be valid is that the distance between the antennas must be greater than the minimum far-field distance, which can be calculated using the following formula, where D is the diagonal of the aperture:

$$d_{\min} = \left(\frac{2D^2}{\lambda}\right). \tag{4.2}$$

For the frequency range of our antenna, which is from 3.95 to 5.85 GHz, the minimum distance must be such that $d_{\min} > 0.25$ m.

At this point it is possible to write power balance that can be used to determine the gain of antenna. If P_g is power output of generator and P_r is received (measured) power, the two powers are related by the next equation[1]:

[1] equation (4.3) is valid for units Decibels

$$P_{\mathrm{r}} = P_{\mathrm{g}} - \alpha \cdot l_1 + G_{\mathrm{x}} - \mathrm{FSL}_{\mathrm{dB}} + G_{\mathrm{r}} - \alpha \cdot l_2. \tag{4.3}$$

Equation (4.3) is one way to calculate the antenna gain, but at some point, the measurement became complicated due to parameters that should be measured, such as attenuation of both cables and distance between antennas. Therefore, it was decided to solve this problem another way that does not require the measurement of cables, etc.

An alternative method of measuring the gain of the antenna involved using a reference antenna with a known gain.

Firstly, the measurement is performed using an antenna whose gain is already known. The symbol used for the gain of this antenna will be G_{test}. Power balance for this case is:

$$P_{\mathrm{r_{test}}} = P_{\mathrm{g}} - \alpha \cdot l_1 + G_{\mathrm{test}} - \mathrm{FSL}_{\mathrm{dB}} + G_{\mathrm{r}} - \alpha \cdot l_2. \tag{4.4}$$

Then the antenna with unknown gain (G_{Tx}) is measured:

$$P_{\mathrm{r_x}} = P_{\mathrm{g}} - \alpha \cdot l_1 + G_{\mathrm{Tx}} - \mathrm{FSL}_{\mathrm{dB}} + G_{\mathrm{r}} - \alpha \cdot l_2. \tag{4.5}$$

For both measurements there is the same power on output of generator and receiving antenna is the same. Both equations have the same unknown parameters and if we subtract (4.4) from (4.5), we get:

$$P_{\mathrm{r_x}} - P_{\mathrm{r_{test}}} = G_{\mathrm{Tx}} - G_{\mathrm{test}}, \tag{4.6}$$

$$G_{\mathrm{Tx}} = P_{\mathrm{r_x}} - P_{\mathrm{r_{test}}} + G_{\mathrm{test}}. \tag{4.7}$$

By using formula (4.7) the unknown gain of antenna can be calculated. However, this method is based on substituting the antenna with a point source known as the "phase center", from which the electromagnetic waves emitted by the antenna are considered to originate. From this point, the waves propagate spherically outward and have the same phase at any point on the spherical wavefront. The distance between two antennas can be considered as the distance between their respective phase centers. Therefore, it is necessary to ensure that the phase center of the antenna remains at the same location during all measurements, so Free Space loss will remain the same.

In these measurements, the antennas were placed in a way that their phase centers were not exactly in the same spot. However, through simulations, it was found that the maximum difference in position[2] was approximately 7 cm. Given that the distance between the antennas was more than 4 meters, it can be claimed that the difference in the position of the phase centers will have an insignificant effect on the free space loss.

Now an example of calculation for horn antenna without any rod will be presented:

Frequency $f = 5$ GHz, $P_{\mathrm{r_x}} = -51.974$ dBm, $P_{\mathrm{r_{test}}} = -47.021$ dBm, $G_{\mathrm{test}} = 13.211$ dBi. Gain of horn antenna on 5 GHz is:

$$G_{\mathrm{Tx}} = -51.974 - (-47.021) + 13.211 = 8.258 \text{ dBi}. \tag{4.8}$$

[2]Positions of phase centers were determined through simulations and are presented in the attachments of this thesis.

4.2 Measurements of gain

In the previous section, a block diagram of the measuring system was presented and the method for determining the antenna gain was demonstrated. This measuring system is shown in Fig. 4.2.

To eliminate the effect of multiple reflections and guarantee the same conditions all measurements were performed in anechoic chamber [3].

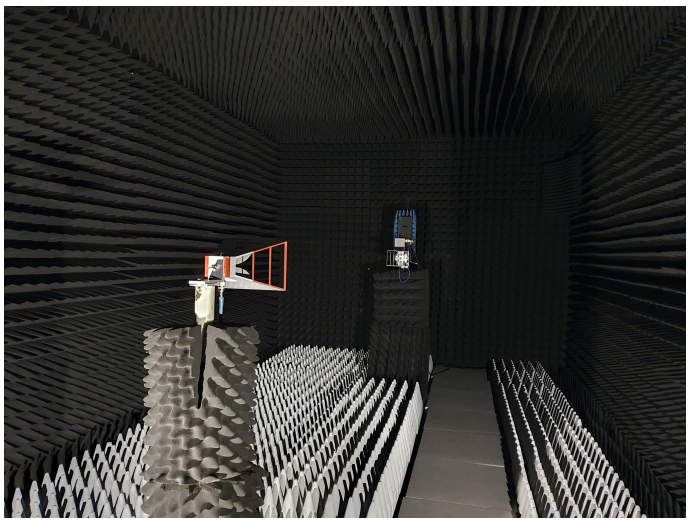

Figure 4.2: Measuring system.

As the first step, an antenna with designated gain was measured (Fig. 4.2). Received power as well as gain of the reference antenna will be used in equation (4.4).

Next, the horn without rod (Fig. 4.3a) is measured, and the measured parameters are then substituted into Equation (4.5).

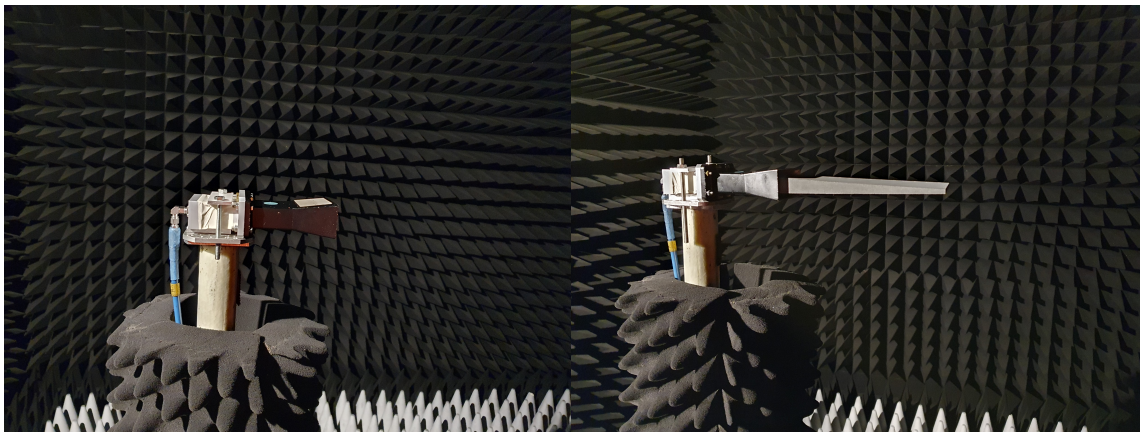

(a) Horn. (b) Horn with the dielectric rod inside.

Figure 4.3: Measurements of gain.

Then the gain of horn without rod was calculated using the formula (4.7). Gain of

[3] Anechoic chamber is a room that is made of absorbing material to prevent reflection of electromagnetic waves

a horn with the dielectric rod (4.3b) was calculated analogically, the only difference was the value of received power, the equation (4.4) was not modified.

The results of the measurements are shown in Fig. 4.4. There are two solid curves that represent the real measurements, and two dashed curves that were obtained from the simulation and were presented in previous chapters (Fig. 3.5). The approximate gain of the horn antenna without the rod, which was presented in 1.8, is also shown on the graph.

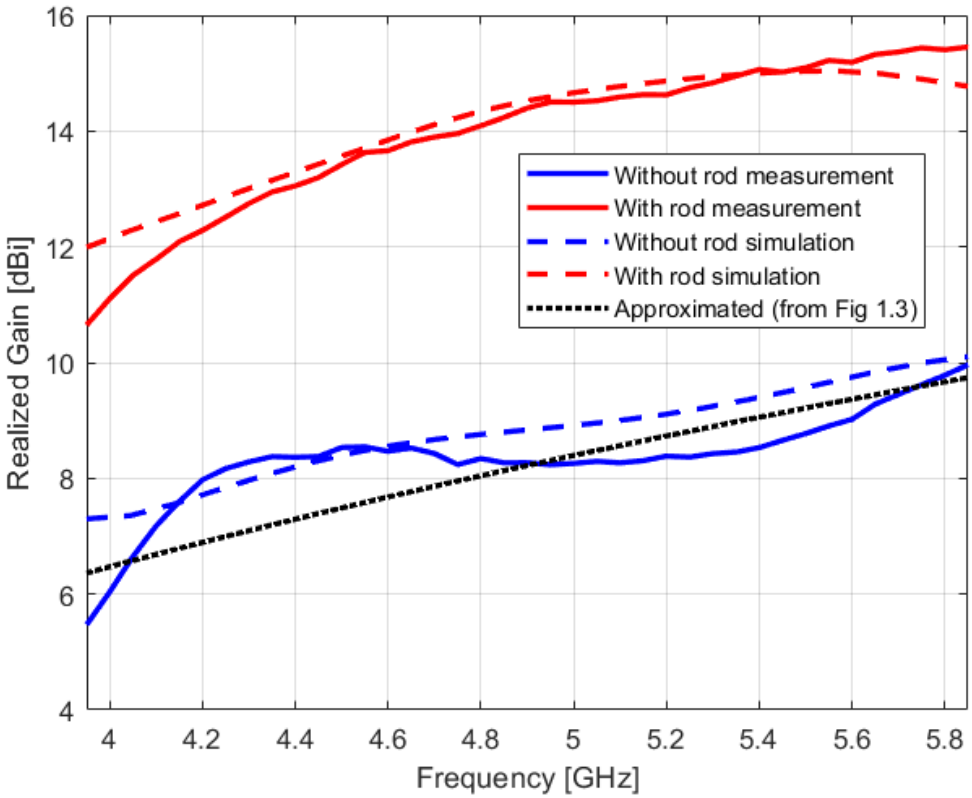

Figure 4.4: Max. gain over frequencies.

Several conclusions can be drawn from Fig. 4.4. First of all, simulations that were performed in CST cannot accurately describe the environment where the antenna was measured, and the measured horn is made of metal that is not a perfect conductor (PEC). Moreover, the mesh that was used in simulations has some accuracy. All these factors contribute to the fact that final measured result is not perfectly matched with the simulation, but despite that, the result of measurement are quite consistent with the simulation results.

Second thing that needs to be clarified is the gain increase and benefit of using dielectric rod. It can be seen from Fig. 4.4 that minimum gain increase is between frequencies 4.1 and 4.5 GHz and is less than 5 dB. With the exception of these frequencies gain grew by an average of 5.5 dB. On some frequencies the increase is more than 6 dB.

Regarding the results of the work, it can be said that the original goal of this thesis was fulfilled, and gain of antenna with dielectric rod has been significantly improved compared to the antenna without the rod.

4.3 Measurements of radiation patterns

This section is dedicated to the measurement of radiation patterns. In fact, the whole measurement procedure was performed exactly the same way as described in previous section. The only one difference was that during the measurement antenna was rotated around the holder. Each antenna was measured twice: E-plane and H-plane.

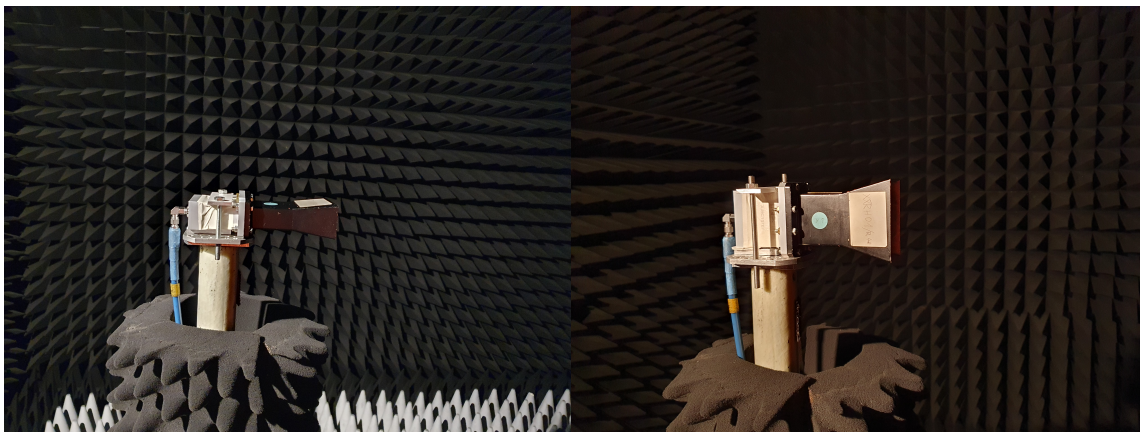

(a) H-plane. (b) E-plane.

Figure 4.5: Horn without rod.

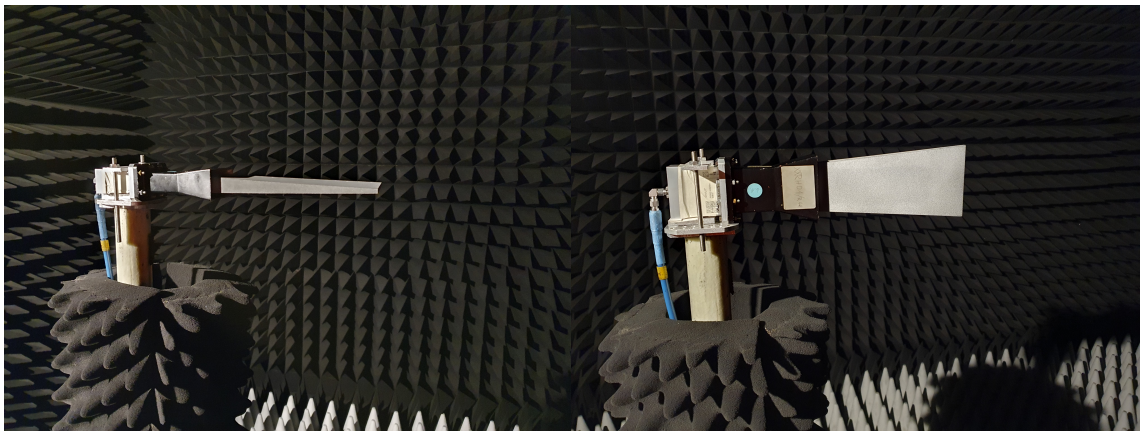

(a) H-plane. (b) E-plane.

Figure 4.6: Horn with the dielectric rod.

The results are shown on upcoming figures. Radiation patterns are shown at a frequency of 4.9 GHz, which is the center of the band. Full lines represent measured data, and there are also dashed graphs that present radiation patterns from simulation.

To summarize the shown results it is necessary to mention that dielectric rod can be used to change radiation pattern of the antenna. And in our case the rod makes antenna more directional: main lobe is narrower and side lobe are suppressed significantly.

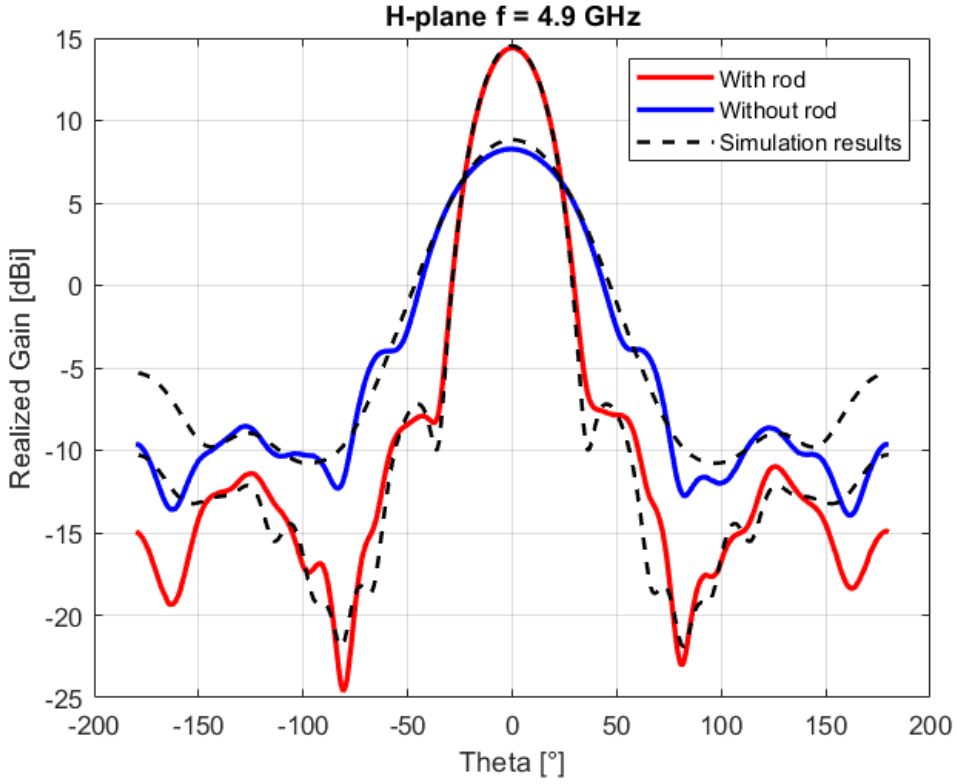

(a) H-plane.

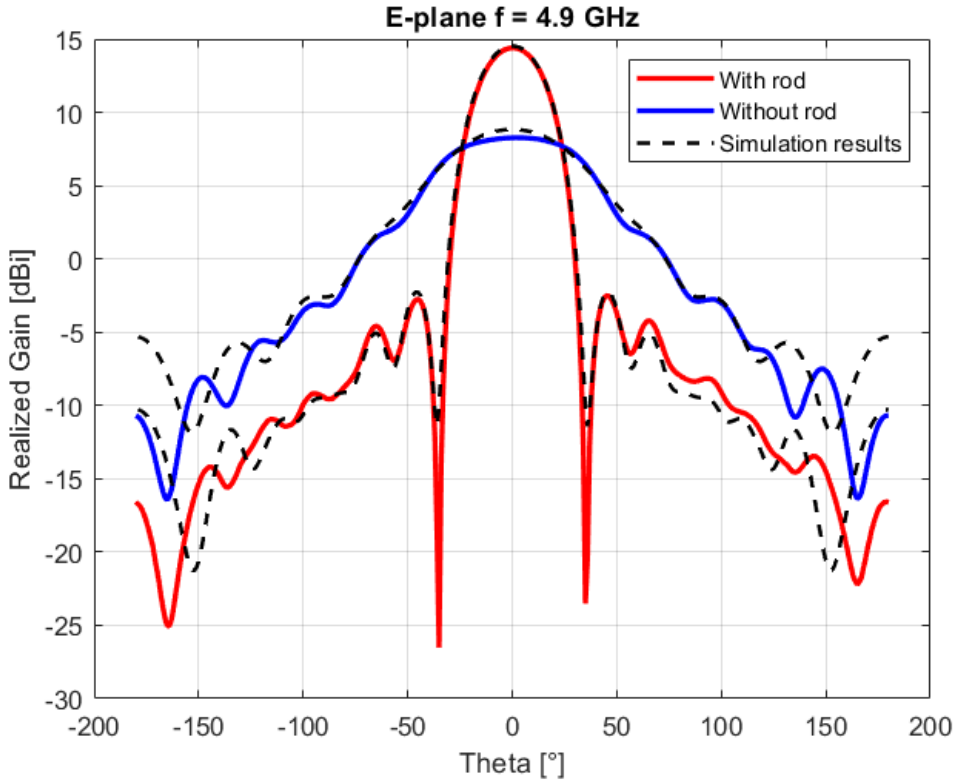

(b) E-plane.

Figure 4.7: Comparison of radiation patterns.

4.4 Reflection coefficient measurements

Last but not least parameter that was measured is reflection coefficient (S_{11}). Its measurement was performed using Vector network analyzer (VNA). To compensate impact of cables and transitions VNA was calibrated using previously mentioned method TRL[4]. Then antenna was pointed to absorbing material to ensure that there will be no reflection other than the reflection from the structure. Upcoming figure 4.8 shows both: measurements results as well as results from simulation that was showed in chapter 3.

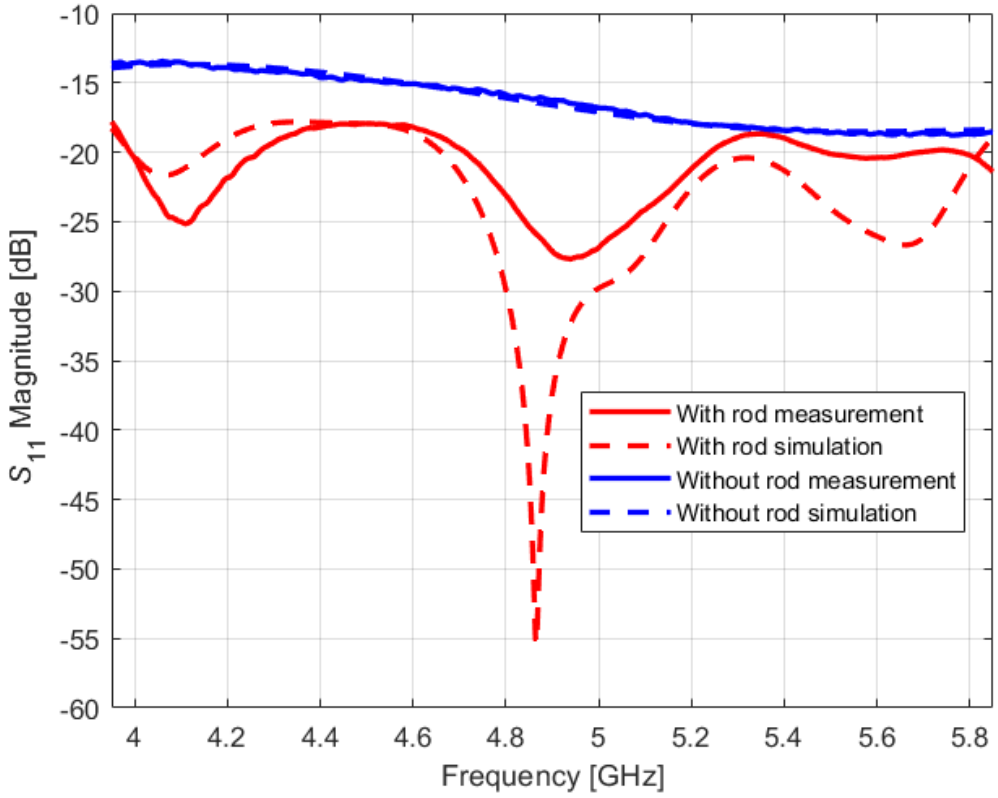

Figure 4.8: Reflection coefficient S_{11}.

As it was said in theoretical part of this thesis S_{11} has an effect on power radiation that cannot be neglected. Reflection coefficient should be as low as possible, so it ensures that structure reflects small amount of energy. For both cases: with rod and without it antenna has a good impedance matching.

4.5 Summary of chapter, comparison of antennas

This section shows comparison of antennas as well as results that were achieved. Upcoming table presents antennas parameters on 4.9 GHz.

Comparing two antennas it is better to start with one of the most important parameters: Realized gain. First of all, gain that was measured almost matches with simulation, there is a small difference between them, but it is not drastic. Regarding

[4]TRL - "True Reflect Line"

to the simulation gain increase was expected to be approximately 5.68 dB, but actual measured increase was 6.13 dB which exceeds the expectations.

Then it is necessary to evaluate how a radiation pattern changed. Measured width of main lobe is closely matched with simulation results and by comparing two antennas it is evident that the presence of a dielectric rod inside the antenna makes it more directional. Side-lobe ratio for both planes got better, which means that side lobes are better suppressed for antenna with the rod. Antenna with the rod radiates less energy towards the back according to results showed in table 4.1. Also, the reflection coefficient S_{11} is presented in this table. However, for better understanding of whether the antenna has good impedance matching, it is better to examine S_{11} across the entire frequency range (see table 4.2).

Table 4.1: Comparison between antennas f = 4.9 GHz.

	Measurements		Simulation	
Parameters	without rod	with rod	without rod	with rod
$\|S_{11}\|$ [dB]	-16.27	-27.13	-16.61	-37.42
Realized gain [dBi]	8.27	14.4	8.84	14.52
Beam-width (H-plane) [°]	56	30	52	30
Beam-width (E-plane) [°]	78	34	74	34
Side-lobe ratio (H-plane) [dB]	-12.15	-22.32	-14.20	-21.70
Side-lobe ratio (E-plane) [dB]	-9.70	-16.91	-11.4	-16.78
Front to Back Ratio (H-plane) [dB]	17.89	29.35	14.15	24.8
Front to Back Ratio (E-plane) [dB]	18.95	30.97	14.15	24.8

Table 4.2: $|S_{11}|$ in the entire frequency range.

	Measurements		Simulation	
Parameters	without rod	with rod	without rod	with rod
$\|S_{11}\|$ [dB]	$<$ -13.4	$<$ -17.7	$<$ -13.7	$<$ -17.8

Now it is necessary to compare impedance matching and so there is reflection coefficient in table 4.2, which is related to the graph 4.8. Regarding to this table it is evident that dielectric rod was designed correctly: impedance matching is not deteriorating; in fact, the reflection coefficient is decreasing, which indicates that less energy is being reflected by the antenna structure itself.

One additional parameter that was improved by inserting the dielectric rod, although it was not the primary aim, is cross-polarization. As mentioned earlier, the dielectric rod can help suppress cross-polarization. Although cross-polarization was not directly measured, there are two figures (Fig. 4.13a and Fig. 4.13b) showing the cross-polarization results at a frequency of 4.9 GHz, and these results are from the simulation.

In summary, based on the previously mentioned observations and results, it can be said that although simulations cannot be perfect and there will always be some degree of uncertainty, the measurement results are quite consistent with the simulation.

Conclusion

The thesis shows its reader the pyramidal horn antenna (WR187) which parameters were improved by inserting dielectric rod. The entire process was showed step by step starting with design recommendations for the rod and explanation of important parameters, followed by material extraction to improve simulation accuracy, preparing for the physical realization of the designed rod, and finally, measuring the antenna with the inserted rod and comparing it to the original antenna.

To summarize the work that was done, the goals of this thesis were achieved. Specifically, an increase in the gain of the antenna with the rod comparing to the original antenna was achieved, with an average increase of 5.45 dB. The reflection coefficient was also improved, with the antenna with the rod having a reflection coefficient of less than -17 dB in the defined band [3.95; 5.85] GHz. Moreover, modified radiation pattern was showed, and based on these results, it was concluded that the final antenna was more directional.

References

[1] TAYEL, Mazhar Basyouni, Tamer Gaber ABOUELNAGA a Azza ELNAGAR. Dielectric loaded Yagi fed dual band pyramidal horn antenna for breast hyperthermia treatment. In: *2018 5th International Conference on Electrical and Electronic Engineering (ICEEE)* [online]. IEEE, 2018, 2018, s. 323-328 [cit. 2022-11-23]. ISBN 978-1-5386-6392-9. Available: doi:10.1109/ICEEE2.2018.8391355

[2] LEE, Hongmin a Hyungsup LEE. A compact dielectric rod-loaded conical horn antenna for millimeter-wave apllications. In: *Proceedings of 2012 5th Global Symposium on Millimeter-Waves* [online]. IEEE, 2012, 2012, s. 182-185 [cit. 2022-11-30]. ISBN 978-1-4673-1305-6. Available: doi:10.1109/GSMM.2012.6314031

[3] SATO, Keisuke, Ichiro OSHIMA a Hisamatsu NAKANO. Rod Antenna for 28-GHz Band Operation. In: *2022 IEEE-APS Topical Conference on Antennas and Propagation in Wireless Communications (APWC)* [online]. IEEE, 2022, 2022-9-5, s. 012-013 [cit. 2022-11-30]. ISBN 978-1-6654-8113-7. Available: doi:10.1109/APWC49427.2022.9900007

[4] MUSTAFA, S. K. a S. YASIR. Design, development and testing of dielectric tapered rod feed for parabolic reflector antenna as an alternate to feed horns. In: *Proceedings of 2013 10th International Bhurban Conference on Applied Sciences and Technology (IBCAST)* [online]. IEEE, 2013, 2013, s. 369-371 [cit. 2022-11-30]. ISBN 978-1-4673-4426-5. Available: doi:10.1109/IBCAST.2013.6512181

[5] ANDO, T., ISAO OHBA, S. NUMATA, J. YAMAUCHI a H. NAKANO. Linearly and curvilinearly tapered cylindrical- dielectric-rod antennas. *IEEE Transactions on Antennas and Propagation* [online]. 2005, **53**(9), 2827-2833 [cit. 2022-11-30]. ISSN 0018-926X. Available: doi:10.1109/TAP.2005.854551

[6] SPORER, Michael, Robert WEIGEL a Alexander KOELPIN. A 24 GHz Dual-Polarized and Robust Dielectric Rod Antenna. *IEEE Transactions on Antennas and Propagation* [online]. 2017, **65**(12), 6952-6959 [cit. 2022-11-30]. ISSN 0018-926X. Available: doi:10.1109/TAP.2017.2764530

[7] JANEZIC, M.D. a J.A. JARGON. Complex permittivity determination from propagation constant measurements. *IEEE Microwave and Guided Wave Letters* [online]. **9**(2), 76-78 [cit. 2022-12-03]. ISSN 10518207. Available: doi:10.1109/75.755052

[8] S. J. Orfanidis, *"Electromagnetic Waves and Antennas"*, 2016 [Online]. Available: https://www.ece.rutgers.edu/ orfanidi/ewa/.

Attachments

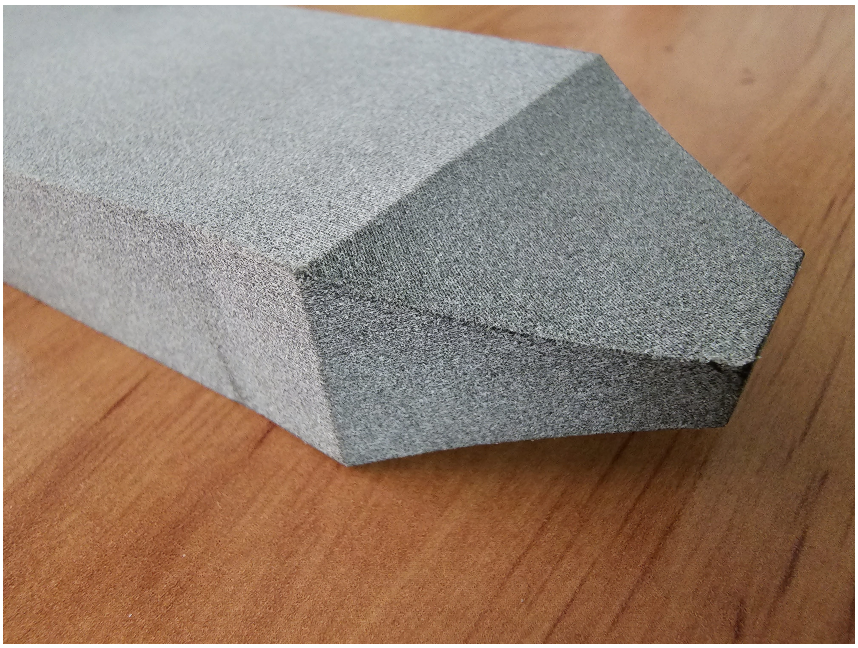

(a) Tapered parts.

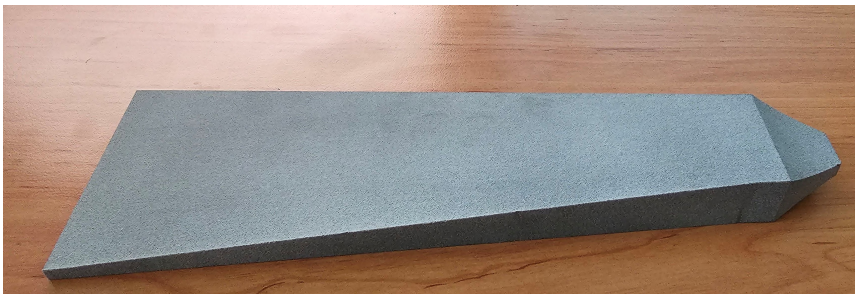

(b) Entire rod.

Figure 4.9: Manufactured dielectric rod

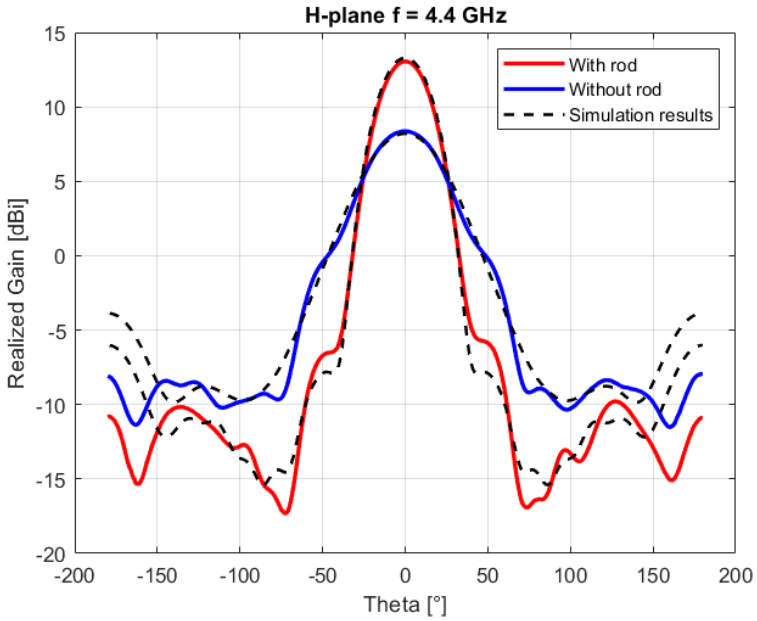

(a) H-plane.

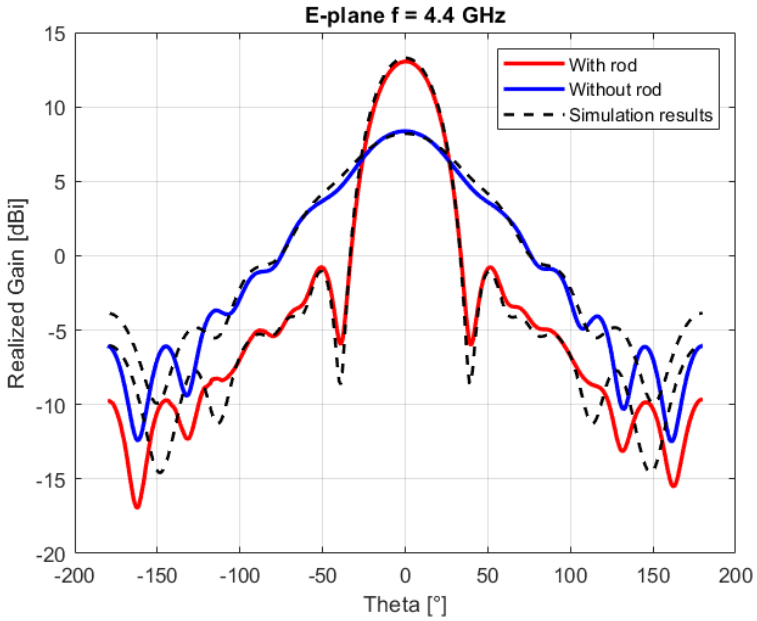

(b) E-plane.

Figure 4.10: Radiation pattern $f = 4.4$ GHz.

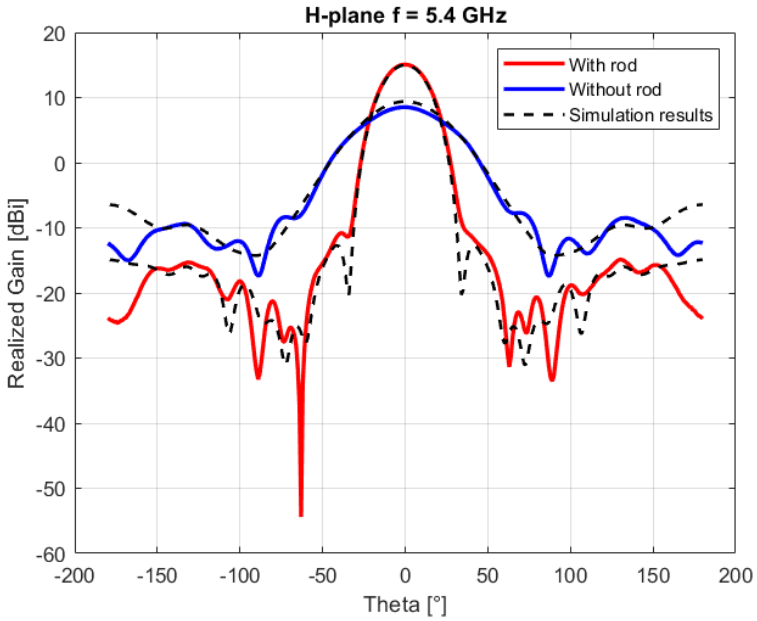

(a) H-plane.

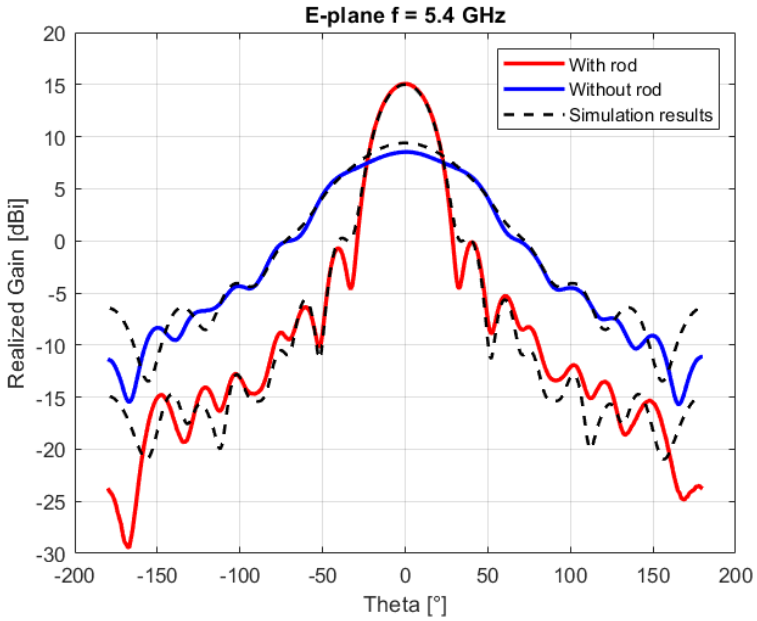

(b) E-plane.

Figure 4.11: Radiation pattern $f = 5.4$ GHz.

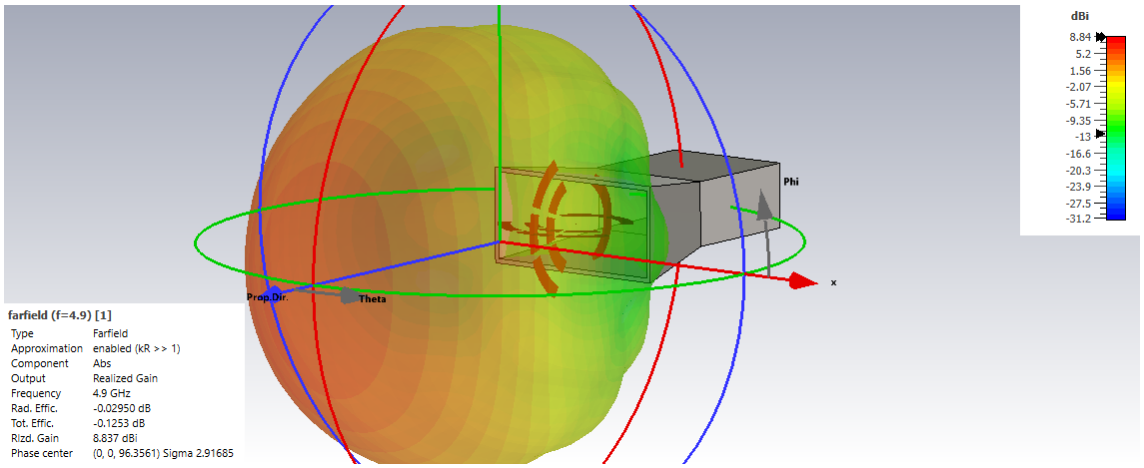

(a) antenna without the rod.

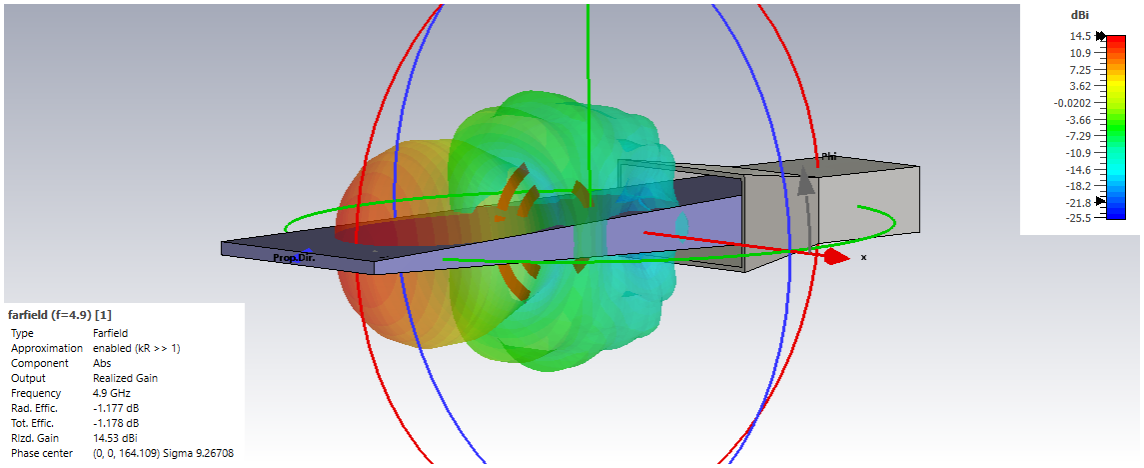

(b) antenna with the rod.

Figure 4.12: Position of the phase center.

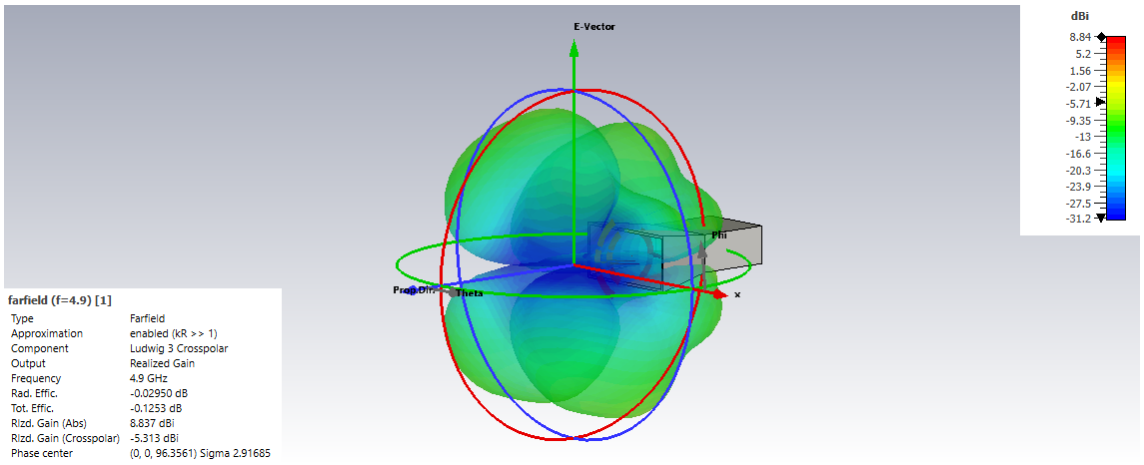

(a) antenna without the rod.

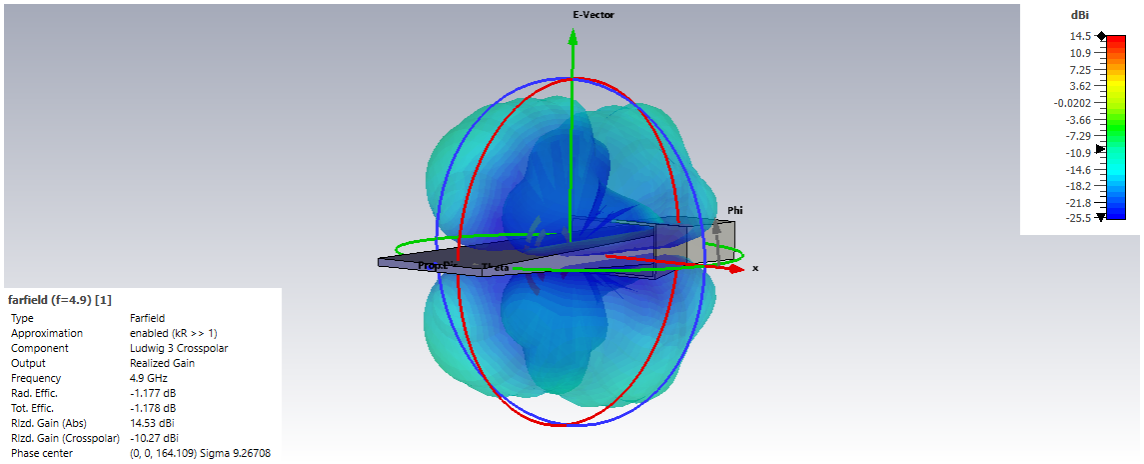

(b) antenna with the rod.

Figure 4.13: Cross-Polarization.

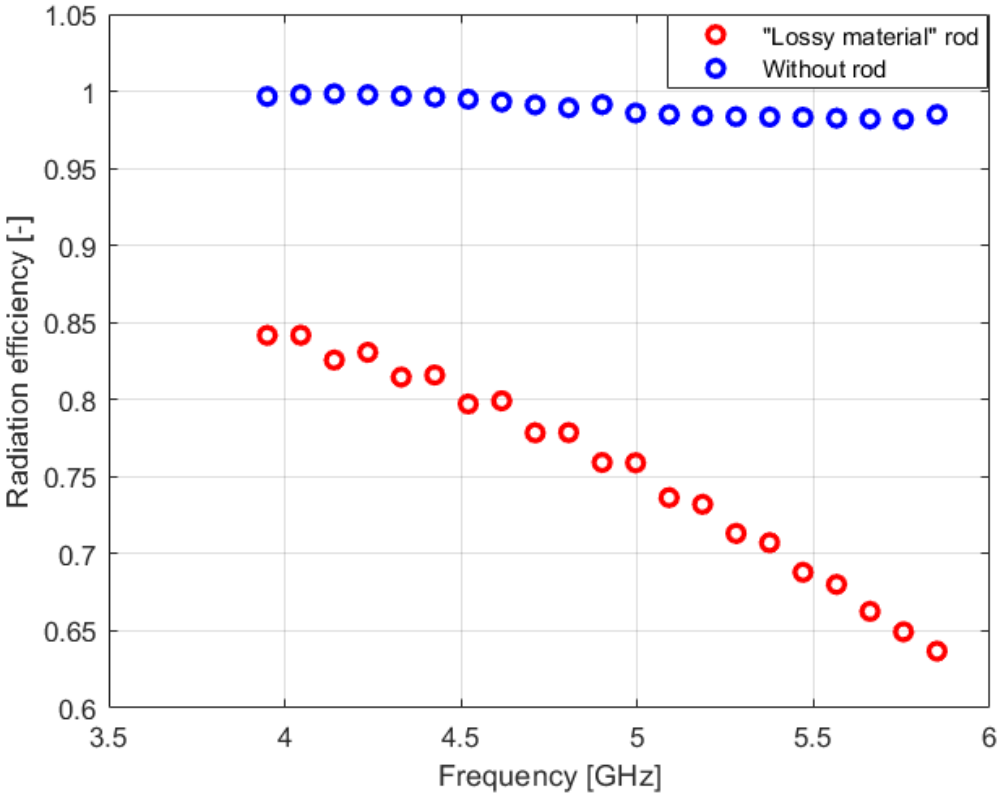

Figure 4.14: Radiation efficiency.